Universidade de Aveiro

Departamento de Ambiente e Ordenamento

2014

Eduardo Forone

Evaluation of the Nazaré canyon´s influence in the maritime agitation of the region through the **SWAN** model application.

Tese apresentada à Universidade de Aveiro para cumprimento dos requisitos necessários à obtenção do grau de Mestre em Ciências do Mar e das Zonas Costeiras, realizada sob a orientação científica do Professor Doutor João Miguel Dias e Doutora Sandra Plecha do Departamento de Fisica da Universidade de Aveiro

Dedico esta tese à toda minha família e à memória da minha avó ...“Vó Luisa”.

JURY

President:

Professora Doutora Filomena Maria Cardoso Pedrosa Ferreira Martins,
Professora Associada, Departamento de Ambiente e Ordenamento da Universidade de Aveiro

Doutor Nuno Alexandre Firmino Vaz,
Bolseiro de Pós-Doutoramento, Centro de Estudos do Ambiente e do Mar (CESAM), Departamento de Física da Universidade de Aveiro

Professor Doutor João Miguel Sequeira Silva Dias,
Professor Auxiliar c/ Agregação, Departamento de Física da Universidade de Aveiro

ACKNOWLEDGMENT

Agradeço aos meus pais, que sempre primaram pela minha educação e foram durante minha vida um modelo a ser seguido, agradeço pelo apoio incondicional, incentivo, amizade e paciência demonstrados.

À todos os amigos conquistados durante essa caminhada, poucos em número mas incomensuráveis em qualidade.

Ao Prof. e orientador João Dias, pela disponibilidade e orientação, pelas indicações e criticas sinceras e pontuais e pela total colaboração no solucionar dúvidas e problemas que surgiram na fase final da tese.

Um agradecimento especial à Drª Sandra Plecha, pela dedicação e disponibilidade na colaboração sempre que por mim foi solicitada. A sua experiência e capacidade de análise relacionada ao SWAN foram fundamentais para a realização desta pesquisa.

ABSTRACT

This dissertation has the main purpose of analyzing the Nazaré canyon influence in the region´s maritime agitation trough the application of the **SWAN** (**S**imulating **WA**ves **N**earshore) mathematical model. To understand the impact of the Nazaré canyon, a synthetic scenario was defined, apart from the real scenario, where the Nazaré canyon was completely fulfilled with sediments and the numerical bathymetry was modified, using a tool from the MOHID modeling system, in a way that the seafloor was like a normal beach brake. The SWAN model was applied for several different forcing conditions and it were analyzed the height, period, direction, length and orbital speed´s results. The results of the simulations performed by SWAN along the Nazaré coast, in different scenarios, confirm the importance of the Nazaré canyon in the wave circulation in this region. In general, all parameters had specific changes, but the changes in wave direction, wave height and orbital velocity, are the ones that showed differences that would cause a highest impact on the wave circulation in the region.

Keywords: Nazaré canyon, SWAN model, significant wave height, Northern beach.

RESUMO

Essa dissertação tem como principal objetivo analisar a influencia do canhão de Nazaré na agitação marítima da região através do modelo matemático SWAN (**S**imulating **WA**ves **N**earshore). Para entender efetivamente o impacto do canhão da Nazaré, para além do cenário real foi criado um outro cenário onde o canhão da Nazaré foi completamente preenchido por sedimentos e a batimetria numérica foi alterada, com o uso de uma ferramenta especifica do sistema de modelagem MOHID, de modo que o fundo oceânico fosse como um “beach brake”. O modelo SWAN foi aplicado com diversos forçamentos diferentes, e foram analisados os resultados de altura, período, comprimento e direção de onda, além da velocidade orbital. Todos os resultados analisados apresentaram mudanças significativas de valores após a alteração na batimetria, o que mostrou a enorme influencia do canhão da Nazaré na agitação marítima, tanto na praia do Norte como na praia da Nazaré. As mudanças na altura e direção das ondas e na velocidade orbital, são as que apresentam maior intensidade e como tal as que causariam uma maior alteração no regime de agitação da região.

Palavras-chave: Canhão de Nazaré, modelo matemático SWAN, altura significativa da onda, praia do Norte.

SUMMARY

FIGURES LIST

TABLES LIST

1. INTRODUCTION

1.1 General considerations

In coastal areas the maritime activity takes on a function of outstanding importance, making therefore crucial to evaluate and predict the state of the sea conditions correctly. The ability to accurately describe the generation and transformation of waves from offshore to the coastal zone is of primary interest for the understanding of existing processes on the coast. It is necessary to take into account that the characteristics of the waves begin to change due to the influence of the bottom as they approach to the coast.

This constant interaction between the sea, the coast and the bottom topography, has a very significant economic and environmental impact. To achieve synergies in the safe and effective management of the planning of the coastline is, therefore essential the knowledge of the maritime agitation.

In this context, the construction of ports, coastal protection structures and areas of shelter or the understanding of coastal morphodynamics (dune erosion and disappearance of beaches) are examples of practical applications where it´s essential to know the characteristics of maritime agitation in the coastal areas.

To characterize correctly the effects of the interaction between the sea and the coast, it is necessary a mathematical model which takes into account the complex physical processes of transformation of the state of the sea which occur on the coast.

This model may be used to simulate the generation of waves by wind on the open ocean and the transformation of their characteristics (height, direction and period) from offshore or from one location on the coast to the place of study.

One of the most widely used models in the generation and forecast of maritime agitation is the **SWAN** model (**S**imulating **Wa**ves **N**earshore) (Booji et al., 1999), which allows the calculation of the evolution of the directional spectrum from the area of wave generation to the coastal zone, thus obtaining

the parameters of the wave characteristic on the interest places.

The SWAN model is a nonlinear spectral model, based on the equation for conservation of wave action, which allows the generation of waves by wind and makes it spread considering various phenomena involved in the propagation of waves: refraction, shoaling, diffraction (roughly), harmonic generation (non-linear interaction between waves).

The present work describes the application of the SWAN model in the maritime area of Nazaré – Portugal (Figure 1.1), and the main idea of this research is to demonstrate the influence of the Nazaré canyon on the region's maritime agitation. Between the data needed for the development of the model, the bathymetry of the ocean floor is the most relevant, and this data was obtained trough Portuguese Hydrographic Institute.

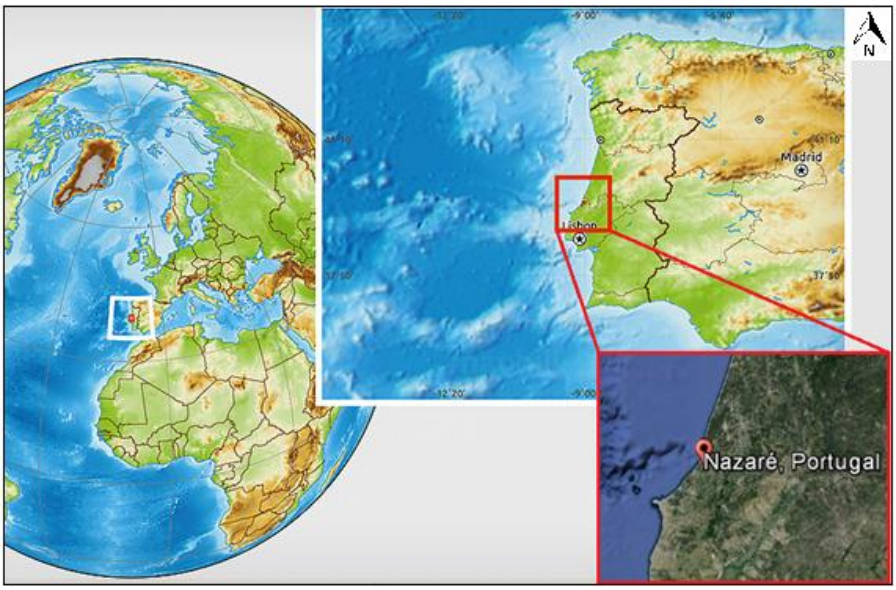

Figura 1.1: Nazaré´s location. Fonte: Maphill 2011©.

The Nazaré area was selected because the Nazaré canyon´s head is situated near shore and causes a significant influence into the hydrodynamic and sediment transport processes leading to particular oceanographic conditions, intrinsically connected with its morphology. To understand the impact of the Nazaré canyon affectively, a synthetic scenario was defined, apart from the real scenario, where the Nazaré canyon was completely fulfilled with sediments and the numerical bathymetry was changed in a way that the seafloor was like a normal beach brake.

This change in bathymetry was done through a specific tool available at the MOHID modeling system.

1.2 Objectives and methodology

The primary goal of this dissertation is to evaluate the influence of the Nazaré canyon in maritime agitation of the region, through the application of the **SWAN** (**S**imulating **WA**ves **N**earshore) mathematical model.

This objective involve the following actions:

- Bibliographical research;
- Analysis of the structure of the data files and of the SWAN model results for the various planned applications;
- Construction of the numerical bathymetry for the study using a tool from the MOHID modeling system;
- Modification of the numerical bathymetry using a specific tool from the MOHID modeling system;
- Sensitivity tests performed with the SWAN model to evaluate the influence of some model parameters (the grid resolution, height and direction of waves) in the numerical results;
- Application of SWAN model in the area adjacent to the Nazaré beach for several different maritime agitation situations;
- Analysis of results through the use of MATLAB;
- Evaluation of potentialities and limitations of the SWAN model to perform this study.

Thus, this study favored the more in-depth knowledge in the area of spread and deformation of waves in coastal areas, both in terms of the physical phenomena involved, either in terms of its numerical modeling. Also allowed familiarization with the conditions of the SWAN model application and the improved use of MATLAB and MOHID and evaluation of the advantages and limitations of the model used.

1.3 State of art

The study of waves is important for the characterization of the marine agitation on the coast and because of the complexity associated with the study of the waves it were created simplifications in order to study the phenomenon, appearing first, the regular waves theory and then the irregular waves theory.

Within the studies of regular waves evolved two theories: the linear wave theory developed by Airy in 1845 and the nonlinear wave theory. The linear wave theory assumes that the water surface is a sinusoidal perfect function and it´s applicable in deep zones and for low amplitude waves.

Nonlinear theory explains the behavior of the waves when the amplitude is larger or when they get close to shallower areas. Stokes (1847, 1880), Bretschneider (1960) and Fenton (1985) are some of the authors that stand out in the development of nonlinear wave theory.

The "spectral" theory which is the most recently used in a large number of wave, is included in the formulation of irregular waves and establishes that the wave generation is best described as a spectral phenomenon. The concept of spectrum is based on Fourier's work and allows to represent a surface as the sum of sines and cosines with different frequencies and oriented in all directions. This is the approach that best describe the spatial variability observed in nature.

The studies of Phillips (1958) and Miles (1957) about the processes of generating waves, (mainly wind field interaction with the surface of the water), and the study of Pierson-Moskowitz (1964) on the wave spectrum properties, created the path for the emergence of the wave models called the 1st generation models.

The 2^{nd} generation of wave models was developed from studies of Hasselmann et al., (1973), which after analysis of data from the Joint North Sea Wave Project (JONSWAP) found that the spectrum is never fully developed due to nonlinear wave-wave interactions. These interactions involve the transfer of energy within the spectrum. An example of a 2^{nd} generation model is the JONSWAP, on which those wave-wave interactions are introduced.

The current 3rd generation models are distinguished from 2nd by the method of wave-wave interaction solution, allowing components (wavelengths) spread by mesh in various directions, growing with the wind or declining over time to establish interactions with the other waves (Stewart, 2002).

Some examples of 3rd generation models are the WAM (Wave Model) and WW3 (Wave Watch 3), developed by the National Oceanic Administration (NOAA) (WAMDI 1988, Komen et al. 1994). The WW3 is a global model of waves (is used to make predictions across the globe) and can be used for grids with 10 km and outside the coastal zone.

Another mathematical model widely disseminated, and which was used for this research, is the SWAN (Simulating Waves Nearshore) of the Faculty of Civil Engineering and Geosciences, Delft University (Booji et al., 1999).

Several studies that used the mathematical model SWAN were already held in the coastal area in question like the observation studies of nonlinear internal waves generated on the Nazaré submarine canyon (Quaresma 2006); research on the sedimentary dynamics in the Nazaré canyon (Ribeiro 2008), in addition to the predictions of maritime agitation and constant monitoring of the canyon. Among all the studies and researchers analyzed, none of them presented directly the influence of the Nazaré canyon at the height of the waves and on the region's maritime agitation.

The Hydrographic Institute, state´s laboratory of the Portuguese Navy, develops research activities related to science and techniques of the sea, contributing to the scientific and technological sea development. The Hydrographic institute is responsible for the MONICAN project, which was created to implement a real time monitoring and operational forecasting capabilities for the Nazaré canyon influence area.

The result of this monitoring shows that the study area is fully exposed to the high energetic NW North Atlantic swell and the locally drift is characterized by a wide directional spreading (from N to SW octants). Offshore incident wave regime is characterized by significant wave height of about 2 m and average peak period of 11 s.

It is clear the importance of the Nazaré canyon in the wave regime of the region. Among all cases of submarine canyons around the world, this is surely one of the most fascinating. Other canyons also have importance in the

scientific world, as the Avilés canyon, Spain, considered the canyon with the highest depth, reaching 4750 m. Another very important canyon is the canyon of the Congo River, known for its impressive range of 800 km. But the largest submarine canyon in the world is located in the Bering Sea, the canyon Zhemchug, which features stunning 11350 km² of drainage area.

In Portugal, the largest submarine canyons are: Portimão Canyon, associated to a geologic fault, the canyon of St. Vincent, also associated with a fault and the Lisbon-Setubal canyons system. The Nazaré canyon is the only one that provide the phenomenon of giant waves.

There are few places around the world where it´s possible to be faced with giant waves as Nazaré. In North America the beaches of Mavericks in California, and Jaws in Hawaii are also world renowned for their power and size, in both cases the wave dissipation is caused by underwater rock formations with unusual shapes.

In Europe, apart from Portugal, France and Ireland are also on the roadmap of big wave surfers. The beaches of Belharra (France) and Mullagamore (Ireland) have reported waves of more than 20 m, the difference is that on both occasions the huge waves are directed against a declivity caused by reefs. The same situation occurs in Teahupoo, Tahiti, where are the most famous and dangerous bench reefs in the world of surfing.

1.4 Stucture of the dissertation

The present work is divided into seven chapters, along with references. In the first chapter is made a general framework of the subject and relevance of research analysis. Chapter 2 presents the theoretical foundations associated with the theme of waves generated by wind, with a brief reference to the linear wave theory and the methodology used for spectral analysis and statistics.

Chapter 3 presents the SWAN model, and describes the energy-balance equation, explaining their terms for the wave energy propagation. Are also referred the numerical methods used by SWAN to integrate the action balance equation, used in order to characterize the evolution of maritime agitation.

Chapter 4 introduces the case study, the specifics that are used for its description (among others definitions of the area of calculus and the boundary conditions). Chapter 5 shows the SWAN application and chapter 6 the results obtained with its interpretation. Finally, chapter 7 presents the final thoughts from this application.

2. WAVE GENERATION

There are several types of sea waves that are associated with different external forcing. The most important and most common type is surface waves. These waves are generated by the wind action over the ocean surface and are surging waves.

As the wind begins to blow over the ocean, turbulence causes pressure fluctuations on the surface of the sea, which produces small waves with lengths almost insignificant. The action of the wind against these small waves causes pressure variations along the wave profile, which causes their growth.

After the waves are formed, they begin to travel over the oceans carrying energy with few losses. These waves move out of their area of generation and acquire a two-dimensional aspect (long crest waves) and are called swell. They are characterized by having high periods (over 10 seconds) and wavelengths greater than 30 times their height. When are formed by local winds, are called by “wind waves”.

The complexity of the processes of generation and propagation of waves is reflected in a non-linearity which makes difficult to solve the movement equation. To find a solution it is necessary to take various simplifications. The most widespread theory is the linear wave theory.

2.1 Linear wave theory

In order to use the linear wave theory is necessary to make various simplifications in the study of sea surface elevation These simplifications pertain to the waves and to the medium in which they propagate:

• Constant water depth (d) and wavelength (λ);

• Movement of two-dimensional waves;

• Constant wave profile in time;

• Incompressible fluid - saltwater specific volume constant;

• The effects of viscosity, surface tension turbulence and Coriolis (due to the movement of the Earth's rotation), are ignored;

• Wave height (*H*) small compared with its length (*λ*) and the water depth (*d*).

The general equations to solve are the equations of conservation of mass and moment. The conservation of mass becomes Laplace's equation, with the adoption of the potential:

$$\frac{\partial^2 \phi}{\partial x^2} + \frac{\partial^2 \phi}{\partial z^2} = 0 \qquad (2.1.1)$$

Where *Φ* represents the speed and *x* and *z* the horizontal and vertical coordinate, respectively, of the system of axes used. For the conservation of momentum, the Bernoulli Equation Not Stationary is adopted:

$$-\frac{\partial \phi}{\partial t} + \frac{p}{\rho} + gz = 0 \qquad (2.1.2)$$

The pressure is represented by *p, ρ* is the specific volume of water and *g* is the gravitational acceleration. To solve the general equations, boundary conditions corresponding to the domain of the solution are necessary:

• Dynamic free surface condition:

$$-\frac{\partial \phi}{\partial t} + g\eta = 0 \text{ , em } z=0 \qquad (2.1.3)$$

On the free surface the pressure is atmospheric.

• Kinematic condition on free surface

$$-\frac{\partial \phi}{\partial t} = \frac{\partial \eta}{\partial t}, \text{ em } z=0 \tag{2.1.4}$$

This condition says that cannot be transported fluid through the surface.

• Kinematic Condition at the bottom of the sea:

$$-\frac{\partial \phi}{\partial z} = 0, \text{ em } z=-d \tag{2.1.5}$$

There can be no flow through the solid boundaries of the ocean. The solution to these equations is as follows:

$$\phi(x,z,t) = \frac{ag}{\omega}\frac{\cosh[k(d+z)]}{\cosh(kd)}\cos(kx-\omega t) \tag{2.1.6}$$

The properties of the wave represented here are:

- *a*: wave height
- *ω*: angular frequency of the wave;
- *k*: wave number

These properties are calculated by means of the following equalities:

$$a = H/2 \tag{2.1.7}$$

$$\omega = {2\pi}/{T} = 2\pi f \tag{2.1.8}$$

$$k = {2\pi}/{\lambda} \tag{2.1.9}$$

Using the dynamic boundary condition on the free surface, is obtained the equation for the surface elevation of the sea:

$$\eta = a\sin(kx - \omega t) \tag{2.1.10}$$

Combining the two boundary conditions on the free surface and the solution obtained previously, results on the relation of dispersion, which provides a unique relationship between the frequency and wave number:

$$\omega^2 = gk\tanh(kd) \tag{2.1.11}$$

Taking a period *T*, the wave advances the equivalent to a wavelength, *λ*. The phase velocity (or spread), which means the speed that each stage of the wave propagates, is by definition equal to:

$$c = \frac{\lambda}{T} = \frac{\omega}{k} \tag{2.1.12}$$

Combining with the relation dispersion equation results in:

$$c^2 = \frac{g}{k}\tanh(kd) \tag{2.1.13}$$

The phase velocity of the wave depends on the depth of the medium in which propagates. For the wavelength, is obtained the following relation:

$$\lambda = \frac{gT^2}{2\pi}\tanh\left(\frac{2\pi d}{\lambda}\right) \tag{2.1.14}$$

As can be understood, this equation may be solved using an iterative calculation. The components of the water particle velocity can be calculated by deriving the speeds.

Applying the solution obtained previously and working on these components, it is possible to get the vertical and horizontal offset of each particle.

Combining the offsets in both axes, is obtained the equation that represents the path of the fluid particles along the wave propagation:

$$\frac{\xi^2}{A^2} + \frac{\zeta^2}{B^2} = 1 \tag{2.1.15}$$

Where ξ and ζ represent the offsets in each direction and A and B are defined by:

$$A = a\frac{\cosh[k(d+z)]}{\sinh(kd)} \tag{2.1.16}$$

$$B = a\frac{\sinh[k(d+z)]}{\sinh(kd)} \tag{2.1.17}$$

From the equation that represents the trajectory of the fluid particles along the wave propagation, is possible to verify that the fluid particles move in closed elliptical orbits. Sea waves are far more complex and can be understood

as the overlapping of several simple waves. The overlapping of waves form groups that move at a speed different from that of the spread of individual waves that form the wave group.

This concept of wave group speed is especially significant because it is equal to the velocity of propagation of wave energy. For two dimensions, the group velocity is determined as follows:

$$c_g \equiv \frac{\partial \omega}{\partial k} \tag{2.1.18}$$

Considering the dispersion relation, the velocity of a wave group is held by the following equation:

$$c_g = \frac{1}{2}\left[1 + \frac{2kd}{\sinh(2kd)}\right]c \tag{2.1.19}$$

2.2 Wave transformation

So far, the results were obtained from linear wave theory in finite-depth water. As it was possible to verify, virtually all the results obtained depend on the water depth.

Thus, it is easy to observe that may be obtained simplifications in situations of deep and shallow water, thus defining the difference between deep and shallow waters, considering limits of transition to the different depths (Figure 2.1). The parameter *d* represents the depth of the water and *L* the wavelength.

When the waves reach the waters of low depth, its shape and direction change. Its speed decreases and the ridges modify their inclination and direction.

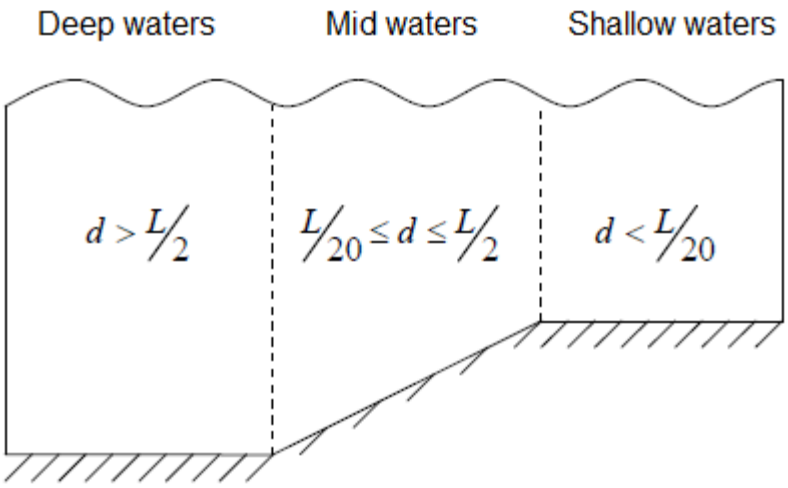

Figure 2.1 : Definition of the various types of depth.

Considering the equations (2.1.13) and (2.1.14), it can be verified that when the period (does not vary with depth) remains constant, but the depth *d* decreases, the speed *c* and the wavelength, *λ*, will also decrease.

This relationship between the speed of the waves and their length (or their period), results from the dispersion relation. In deep water, the waves propagate faster than in shallow waters. So when a group of waves travels outside their area of generation, longer waves will travel faster and the shorter more slowly. This causes the wave group separation based on their wavelengths. Therefore the waves field will gradually disperse.

2.3 Approaches

The dispersion relation of the waves depends on a trigonometric function: hyperbolic tangent. This function has the behavior shown in Figure 2.2.

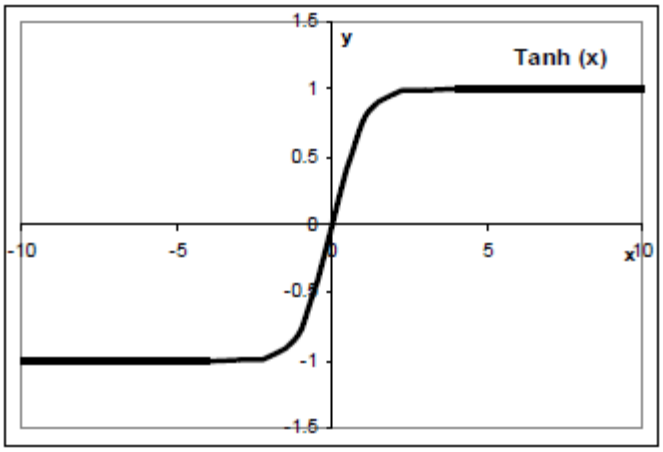

Figure 2.2 : Hyperbolic tangent of a function x.

For deep water, $d > \lambda$, i.e., the depth is much larger than the wavelength. Considering the wave length equation, this means that $kd > 1$. Looking at the behavior of the function, for deep waters, it has the following simplification:

$$\tanh(kd) \approx 1 \tag{2.3.1}$$

The reasoning is the same for shallow waters. Whereas $d << \lambda$ that means $kd << 1$, and so :

$$\tanh(kd) \approx kd \tag{2.3.2}$$

From these results, it is possible to get the approximations for the wave parameters, taking into account the depth (Table 2.1):

Table 2.1: Main approaches for different depth.

	Deep waters	Shallow waters
Phase Velocity (equation (2.1.12))	$c = g/\omega$	$c = \sqrt{gd}$
Group Velocity (equation (2.1.19))	$c_g = c/2 = g/2\omega$	$c_g = c = \sqrt{gd}$
The dispersion relation (equation 2.1.11))	$\omega^2 = gk$	$\omega^2 = gk^2 d$

Analyzing the equations, which represent displacements in each direction of the path of the fluid particles along the wave propagation, it turns out that the displacement of a particle of water also depends on the depth. Thus, the equation that represents the movement of the water particles according to Linear Theory, can be individualized for both types of depth. In the case of deep water (kd > 1), the quantities A and B take equal values and thus the particle trajectory becomes circular.

2.4 Transformation processes

The transition between different depths causes changes in the profile of the wave. As already described, the wave characteristics change with depth, and these changes originate certain physical phenomena responsible for the transformation of the waves as they approach the coast.

2.4.1 Shoaling

The length of the waves decreases with depth. The energy between two consecutive crests remains constant during its propagation. Thus, when the wavelength decreases, the wave height increases considering that the amount of energy carried is the same on a smaller free surface area. Knowing that there is equality of power flow between two wave fronts, becomes:

$$\left(E_a c_{g_a}\right).b_a = \left(E_b c_{g_b}\right).b_b \tag{2.4.1.1}$$

Where *b* represents the wave fronts. Knowing the energy transported per unit area by a wave:

$$\overline{E} = \frac{1}{8}\rho g H^2 \tag{2.4.1.2}$$

Is obtained the following relationship between wave heights that propagate in different water depths:

$$H_b = H_a \sqrt{\frac{c_{g_a}}{c_{g_b}}} \sqrt{\frac{b_a}{b_b}} \qquad (2.4.1.3)$$

The subindice *b* represents the wave front in shallow water and *a* in deep water.

2.4.2 Refraction

The most significant environmental feature of the near-shore region is that water depths are shallow and change rapidly. The shallow depths mean that the ocean surface waves can “feel” the bottom, which causes a change in how waves move, or propagate along the surface, and a change in the shape at the waves as the depth gets shallower.

A general rule is that a wave will start to be affected by water depth when the depth is less than or equal to half the wavelength. At this point, two main effects will start to occur. The first effect is that the wave will start to turn toward shore so that eventually the wave crests become parallel to the shoreline regardless of the angle at which they started in deeper water. This turning is referred to as wave refraction, and it occurs more rapidly for regions where the depth is getting shallow faster than in region where the depth change is gradual.

Naturally, if the waves start in deep water with their crests parallel to shore, then wave refraction cannot be seen since there is no turning. The second effect is that the wavelength and amplitude of the waves change as depth gets shallower

This process can be represented by Snell's law:

$$\frac{\sin\theta}{c} = \frac{\sin\theta_0}{c_0} \qquad (2.4.2.1)$$

Where c and c_0 correspond to wave speeds in shallow water (near the coast) and in deep water, respectively, and θ is the angle of incidence of the wave, i.e. the angle that the crest of the wave make with the beach line.

2.4.3 Breaking

As the wave propagates to shallower areas, friction from the bottom starts to slow down the waves orbital motion while holding the upper part of its initial velocity. The waves start to lean forward and when this tilt reaches a maximum value, the wave bursts.

This maximum value represents the criterion of breaking waves as already been proposed by several authors. McCowan (1894) suggested that at the time when ruptured, the waves have the following height:

$$H_b = kh_b \tag{2.4.3.1}$$

Being $k = 0.78$

Iribarren parameter allows to classify the kind of breaking waves: spilling, plunging, collapsing and surging.

$$I_r = \frac{\tan\beta}{\left(H/\lambda\right)^{1/2}} \tag{2.4.3.2}$$

Where β represents the slope of the beach. Then the breaker types dependence on the Iribarren number (either ξ_0 or ξ_b) is approximately:

Tabel 2.2: The breaker types dependence on the Iribarren number.

Breaker type	**ξ_0–range**	**ξ_b–range**
Surging or collapsing	$\xi_0 > 3.3$	$\xi_b > 2.0$
Plunging	$0.5 < \xi_0 < 3.3$	$0.4 < \xi_b < 2.0$
Spilling	$\xi_0 < 0.5$	$\xi_b < 0.4$

2.4.4 Diffraction

Diffraction involves a change in direction of waves as they pass through an opening or around a barrier in their path. Water waves have the ability to travel around corners, around obstacles and through openings. This ability is most obvious for water waves with longer wavelengths. Diffraction can be demonstrated by placing small barriers and obstacles in a ripple tank and observing the path of the water waves as they encounter the obstacles. The waves are seen to pass around the barrier into the regions behind it; subsequently the water behind the barrier is disturbed. The amount of diffraction (the sharpness of the bending) increases with increasing wavelength and decreases with decreasing wavelength. In fact, when the wavelength of the waves is smaller than the obstacle, no noticeable diffraction occurs.

Diffraction of water waves is observed in a harbor as waves bend around small boats and are found to disturb the water behind them. The same waves however are unable to diffract around larger boats since their wavelength is smaller than the boat.

2.4.5 Reflection

Surface waves can be bent (refracted) or bounced back (reflected) by solid objects. Waves do not propagate in a strict line but tend to spread outward while becoming smaller. Where the wave front is large, such spreading cancels out and the parallel wave fronts are seen traveling in the same direction. Where the lee shore exists, such as inside the harbor or behind an island, waves can be seen to bend towards where the waves are. In the lee of islands, waves can create an area where they interfere, causing steep and hazardous seas.

When approaching the gently sloping shore, waves are slowed down and bent towards the shore. When approaching the steep rocky shore, waves are bounced back, creating a 'confused sea' of interfering waves with twice the

height and steepness. Such places may become hazardous to shipping in sea otherwise with acceptable conditions.

2.5 Waves spectral representation

The observation of the state of the sea shows that this rarely can be represented by a simple sine. Its irregularity shows that is formed by several waves of different amplitudes, lengths and periods. To better represent the surface of the sea, overlapping of multiple sine waves with different sequences and stages is necessary.

Using the Fourier series, and knowing that the elevation of the sea surface considering only one sinusoidal wave is represented by:

$$\eta(x,t) = a\cos(kx - \omega t + \varepsilon) \tag{2.5.1}$$

Where *a* represents the amplitude of the wave, *k* the wave number, *ω* the angular frequency and *ε* the lag of the wave.

The elevation of the sea surface can be represented as a superposition of multiple harmonics travelling in several directions and frequencies:

$$\eta(x,y,t) = \sum_{i=1}^{N} a_i \cos(k_i x\cos\theta_i + k_i y\sin\theta_i - \omega_i t + \varepsilon_i) \tag{2.5.2}$$

For this irregular sea state, and taking into account the transported energy equation, energy per unit area of the wave system is:

$$\overline{E} = \frac{1}{8}\rho g\sum_{i=1}^{N} H_i^2 \tag{2.5.3}$$

Considering a fixed point in space, the surface elevation equation as a function of time is:

$$\eta(t) = \sum_{i=1}^{N} a_i \cos(\omega_n t + \varepsilon_i) \tag{2.5.4}$$

The total energy of the wave per unit area, can also be given by:

$$E = \frac{1}{2}\rho g \int_{-\infty}^{+\infty} [\eta(t)]^2 dt \tag{2.5.5}$$

The variance of $\eta(t)$ over a period of time T, is represented by:

$$\overline{[\eta(t)]^2} = \frac{1}{T}\int_0^T [\eta(t)]^2 dt \tag{2.5.6}$$

Which can be written in terms of average energy per unit area:

$$\overline{E} = \frac{1}{2\pi}\rho g \int_{-\infty}^{+\infty} \frac{[a(\omega)]^2}{T} d\omega \tag{2.5.7}$$

The power spectral density is, by definition, equal to:

$$S(\omega) = \frac{[a(\omega)]^2}{\pi T} \tag{2.5.8}$$

The integral of the curve defined by $S(\omega)$ provides the total system wave power:

$$E = \frac{1}{2}\rho g \int_{-\infty}^{+\infty} S(\omega) d\omega \tag{2.5.9}$$

2.6 The variance spectrum parameters

The propagation of a wave system is represented by the sum of a large number of wave components. These components are considered random

processes and statistically independent. Thus, it can be assumed that the elevation of the surface of the sea is a Gaussian process. Thus, the probability distribution of the surface elevation is given by:

$$p(\eta) = \frac{1}{\sqrt{2\pi E}} \cdot \exp\left(\frac{-\eta^2}{2E}\right) \tag{2.6.1}$$

From the variance spectrum, it is possible to remove the *E* parameter necessary for its characterization. This parameter corresponds to the moment of order 0, which will be seen in the next equation.

The peak frequency, *ωp*, permits to estimate the peak period:

$$T_p = \frac{2\pi}{\omega_p} \tag{2.6.2}$$

The definition of other parameters that can characterize the state of the sea, is established starting from the concept of moment of order *n* of the spectrum:

$$m_n = \int_0^\infty \omega^n S(\omega) d\omega \tag{2.6.3}$$

Like this:

Significant Height.

$$Hs = 4\sqrt{m_0} \tag{2.6.4}$$

The Average period (corresponding to the average frequency of the spectrum).

$$T_{m01} = 2\pi \frac{m_0}{m_1} \tag{2.6.5}$$

Average period of ascendants zeros.

$$T_z = 2\pi\sqrt{\frac{m_0}{m_2}} \tag{2.6.6}$$

Average period between peaks.

$$T_c = 2\pi\sqrt{\frac{m_2}{m_4}} \tag{2.6.7}$$

It´s possible to calculate another parameter that allows to sort the irregularity of the sea state:

$$\varepsilon = \sqrt{1-\left(\frac{T_c}{T_z}\right)^2} \tag{2.6.8}$$

This value must be between 0 and 1. The lower limit corresponds to a fairly regular sea state, defined by the narrowband spectrum, while the upper limit relates to very irregular waves, with a broadband spectrum. This value is very important because some of the parameters calculated across the spectrum are only approximations to narrow-band spectra. Generally, it is considered that a narrowband spectrum is obtained when $\varepsilon < 0.6$.

2.7 Parametric wave spectra

From the analysis of the wave records were developed several theoretical spectra, that seek to represent the real spectrum of wave and depend on a number of parameters.

There are two theoretical models that are the most widely used to characterize sea states: Pierson-Moskowitz and JONSWAP spectrum.

The first model characterize a fully developed sea state and it is subject to the natural process of the wind. Thus, the transmission of energy between the two means (wind and sea) reaches saturation and the system is in balance.

$$S(\omega) = \frac{\alpha g^2}{\omega^5} \exp\left[-0.74 \left(\frac{\omega U_w}{g} \right)^{-4} \right] \tag{2.7.1}$$

Where:

- $\alpha = 0.0081$;
- ω - Angular frequency;
- U_w – Wind speed

The peak frequency of the spectrum can be calculated using the following formula:

$$\omega_0^2 = 0.161 \frac{g}{H_s} \tag{2.7.2}$$

The second theoretical spectrum, JONSWAP spectrum, was developed based on the study of wave regime data obtained from the North sea. This represents the sea states without the wind action This spectrum is given by:

$$S(\omega) = \frac{\alpha g^2}{\omega^5} \exp\left[-1.25 \left(\frac{\omega}{\omega_0} \right)^{-4} \right] \cdot \gamma^{\exp\left[-\frac{(\omega-\omega_0)^2}{2\sigma^2\omega_0^2} \right]} \tag{2.7.3}$$

Where:

- γ - Peak parameter;
- σ_H - Shape parameter.

The parameters ω_0 and a are calculated knowing the distance over which the wind is felt. It should be mentioned that this spectrum is equal to that of the Pierson-Moskowitz when $\gamma = 1$.

3. SWAN MODEL

The **SWAN** (***S****imulating* ***Wa****ves* ***N****earshore*) model, was developed at the Technical University of Delft (TUDelft), Holland; is a third-generation numerical model which is used to represent the generation and propagation of waves in coastal areas, from data on boundary conditions, wind fields, currents and bathymetry.

The SWAN, based on the resolution of the variance spectral balance equation, arises from the need to complement the third-generation models developed essentially for operational applications in deep waters. The model propagates, in the geographical domain, the directional spectrum and consequently, calculates the evolution of the waves generated by the wind in coastal areas.

The mathematical formulation of the model involves not only the phenomena of generation, dissipation and non-linear interaction between four waves, as well as the existing processes in shallow waters, such as the dissipation due to friction from the bottom, nonlinear interaction between three waves and surf-induced decrease in depth.

3.1 Mathematical structure of the model

The following topics will described the theoretical fundaments of the SWAN model, in particular, the energy balance equation, and their energy propagation terms, the way the wind field is introduced, consideration of non-linear interactions between the waves and the formulation used for the energy dissipation.

3.1.1 Energy balance equation

Under the conditions described in Chapter 2, the variance spectrum provides all the necessary information to the statistical characterization of the sea surface. The spectral energy balance equation formulated in Eulerian coordinates is expressed by:

$$\frac{\partial E(f,\theta;x,y,t)}{\partial t}+\frac{\partial c_{g,x}E(f,\theta;x,y,t)}{\partial x}+\frac{\partial c_{g,y}E(f,\theta;x,y,t)}{\partial y}+\frac{\partial c_{\theta}E(f,\theta;x,y,t)}{\partial \theta}=S(f,\theta;x,y,t) \quad (3.1.1.1)$$

This equation includes phenomena such as the shoaling, which is implicit in the group velocity as a function of depth, and the refraction, expressed by the change direction speed. Diffraction is not considered and the θ variable refers exclusively to the effect of refraction.

When considering maritime currents it is necessary to consider the transfer of energy between the waves and the currents and the effects associated with this phenomenon. In this case is defined the density of action $N(x, t,\sigma,\theta)$, space x and time t, since this is preserved in the presence of currents, contrary to energy.

$$N(\sigma,\theta)=\frac{E(\sigma,\theta)}{\sigma} \quad (3.1.1.2)$$

Where σ is the relative frequency and θ the direction of the wave.

Therefore, the balance action equation, set to Cartesian coordinates, is expressed by:

$$\frac{\partial N(\sigma,\theta;x,y,t)}{\partial t}+\frac{\partial c_{g,x}N(\sigma,\theta;x,y,t)}{\partial x}+\frac{\partial c_{g,y}N(\sigma,\theta;x,y,t)}{\partial y}+\frac{\partial c_{\theta}N(\sigma,\theta;x,y,t)}{\partial \theta}+\frac{\partial c_{\sigma}N(\sigma,\theta;x,y,t)}{\partial \sigma}=\frac{S(\sigma,\theta;x,y,t)}{\sigma} \quad (3.1.1.3)$$

The first term represents the rate of change of density of local action in time, the second and third represent the spread of action in geographical space (with speeds of propagation, C_{gx} C_{gy}), the fourth term refraction-induced currents and varying depth and finally the fifth sets the relative frequency change due to variations in depth and currents. The latter is null in the absence of currents.

The quantities c_q and c_s represent the propagation velocities in spectral space. The term present on the right side of the equation, $S(\sigma,\theta)$, covers all of the sources or sinks terms associated with the physical phenomena that generate, dissipate or redistribute the energy of the ondulation. $S(\sigma,\theta)$ can be subdivided in power generation due to wind $S_{in}(\sigma,\theta)$, in the non-linear interactions $S_{nl}(\sigma,\theta)$ and in energy dissipation $S_{diss}(\sigma,\theta)$.

$$S(\sigma,\theta) = S_{in}(\sigma,\theta) + S_{nl}(\sigma,\theta) + S_{diss}(\sigma,\theta) \qquad (3.1.1.4)$$

The term $S_{diss}(\sigma,\theta)$ describes three phenomena: friction from the bottom - $S_{diss\ b}(\sigma,\theta)$ surf induced by the decrease of the deep - $S_{dissbr}(\sigma,\theta)$, and partial breaking - $S_{diss\ w}(\sigma,\theta)$.

3.1.2 Terms of propagation

When the oceanic wave propagates from the generation area till the place where the dissipation of energy occurs, usually in coastal areas, the change in the depth affect the characterization of the maritime agitation, resulting in phenomena like the shoaling, refraction, diffraction, the interaction between the currents and waves and the shoaling.

Having in mind the dispersion relationship ($\sigma^2 = gk\tanh(kh)$) it works out that the wavelength and speed decrease with the depth. The effect of shoaling has as consequence the height increase, being that in the absence of currents, the corresponding frequency remains constant. To proceed to the calculation of refraction it should be referred the Eulerian approach that discretize the geographical space in multiple cells.

This approach requires the rate of the wave direction change. As mentioned, the waves are affected in their direction, frequency and amplitude when they propagate in a medium with currents.

The linear theory is valid for the analysis of this new medium, since it considers the depth and currents constants in space and time.

The absolute frequency ω results from the sum of two portions: the relative frequency and the product between the wave number *k* and the vector representing the speed of current *u.*

$$\omega = \sigma + \vec{k}.\vec{u} \qquad (3.1.2.1)$$

Where σ is the frequency in the dispersion relation.

When considering that the depth and the speed of currents are constants, it induces that relative frequencies are also constant. Similarly, if the depth or speed change, the frequency also varies.

Taking into account the presence of currents, are adopted the following aspects in the SWAN model for the propagation velocities of wave energy $c_g + u$, $c\theta$ and $c\sigma$ in space *x,y*, in space defined by θ and space of relative frequency σ:

$$\frac{dx}{dt} = c_g + \bar{u} = \frac{1}{2}\left[1 + \frac{2kh}{\sinh(2kh)}\right]\frac{\sigma\bar{k}}{|\bar{k}|^2} + \bar{u} \qquad (3.1.2.2)$$

$$\frac{d\theta}{dt} = c_\theta = -\frac{1}{k}\left[\frac{\partial\sigma}{\partial h}\frac{\partial h}{\partial m} + \bar{k}\frac{\partial\bar{u}}{\partial m}\right] \qquad (3.1.2.3)$$

$$\frac{d\sigma}{dt} = c_\sigma = \frac{\partial\sigma}{\partial h}\left(\frac{\partial h}{\partial t} + \bar{u}\nabla h\right) - c_g\bar{k}\frac{\partial\bar{u}}{\partial s} \qquad (3.1.2.4)$$

Where *s* is the displacement in the direction of propagation, *h* the depth and *m* the offset in the perpendicular. The operator *d/dt* refers to the total derivative within the propagation of wave energy.

$$\frac{d}{dt} = \frac{\partial}{\partial t} + (c_g + \bar{u})\nabla_{\bar{x}} \qquad (3.1.2.4)$$

3.1.3 Forcing by the wind field

There are two types of approach to describe the mechanisms of transfer of energy from the wind to the free sea surface. One considers a growth of linear wave energy at the time, while another argues that the process of interaction between the wind and the waves results in exponentially growth.

With the contribution of the theories mentioned, it is described the effect of the wind on the free surface:

$$S_{in}(\sigma,\theta) = A + BE(\sigma,\theta) \qquad (3.1.3.1)$$

The term *A* describes the linear growth of energy in time, due to atmospheric pressure fluctuations induced by the wind. The second term is relative to the exponential growth of energy.

Both depend on the frequency and wave direction, speed and wind direction.

3.1.4 Non-linear interaction of waves

Several studies have shown that it is essential to consider the non-linear interactions between four deepwater waves, since they dominate the evolution of the spectrum. Due to interactions with four waves, there is transfer of energy from the peak of the spectrum to lower frequencies and partly to higher frequencies.

Non-linear interactions between four waves, thus play a significant part in the redistribution of spectrum energy.

The calculation of nonlinear interactions between four waves involves a Boltzman constant integral (Komen et al., 1994).

The numerical models, including the SWAN, use approximations for this calculation, such as "Discrete Interaction Approximation" (DIA), (Rogers et al., 2001). In shallower waters, non-linear interactions between three resonant waves become relevant in the evolution of the spectrum, transferring energy from the lower frequencies to higher frequencies, resulting in super harmonics (SWAN Team,2008).

This energy transfer process can be done in very short distances, changing the configuration of the spectrum considerably.

The SWAN model uses the term concerning non-linear interactions of three waves, $S_{nl3}(\sigma,\theta)$, through the approach “Lumped Triad Approximation” – LTA (Eldeberky, 1996).

3.1.5 Partial waves – Whitecapping

The partial breaks depends on the slope of the wave. In the SWAN model, similarly to the others 3rd generation models currently used, partial breaking is formulated using the following expression:

$$S_{ds,w}(\sigma,\theta) = -\Gamma \sigma_m \frac{k}{k_m} E(\sigma,\theta) \qquad (3.1.5.1)$$

The coefficient Γ depends on the slope, k is the wave number and σ_m, k_m represent, respectively, the average frequency and the number wave average.(WAMDI group, 1988).

O coeficiente Γ depende da declividade, k é o número de onda e σ_m e k_m representam, respectivamente, a frequência média e o número de onda médio (WAMDI group, 1988).

The value of Γ is estimated using the equation of energy balance for a complete state of development, and is dependent on the type of formulation used for the representation of the winds. As are used two expressions, the coefficient Γ will take two different values.

3.1.6 Bottom friction

In shallower waters orbital movements of the liquid particles stretch to the bottom. The bottom friction arises in the context of the transfer of energy, as a result of the interaction of the particles with the bottom. Several studies were performed in order to create a good characterization of this phenomenon.

The SWAN model has three formulations available for friction in the background. All of them can be expressed as follows:

$$S_{ds,b} = -C_b \frac{\sigma^2}{g^2 \sinh^2 kh} E(\sigma,\theta) \tag{3.1.6.1}$$

Where C_b is an inherent friction coefficient.

3.1.7 Shoaling induced by the seafloor

As the depth decreases, the energy of the wave is concentrated in such a way that at a given moment when the wave breaks, quickly dissipates energy. In the SWAN model the equation used to describe the shoaling effect induced by the bottom is expressed by:

$$S_{ds,br}(\sigma,\theta) = \frac{D_{tot}}{E_{tot}} E(\sigma,\theta) \tag{3.1.7.1}$$

D_{tot} being the average wave energy dissipation per unit horizontal surface (Ris, 1997).

3.2 Numerical implementation

The waves generated by the wind are random in nature, they have multiple time scales which add difficulty for the 3rd generation models. Thus, it is necessary to distinguish the numerical errors of errors derived from physical processes modeling. To use a numerical wave model, one of the biggest concerns is the spent calculation time. In this sense, the choice of numerical

inputs for the waves propagation through the geographical space is very important, and must satisfy criteria of stability, consistency and convergence (Smith, 1978).

Usually, for deep water, models that are based on schemes with finite differences are used. However, for applications in shallow waters, it´s noted that the time interval used should be very small, making the calculations economically unviable. Such implication is derived from the Courant Fredrik-Levy (CFL) condition, which states that the wave energy cannot propagate in the directions *x* and *y* through more than a geographic cell Δx and Δy , which limits the propagation velocities in a numeric space.

$$\Delta t \leq \frac{\Delta x}{c_{g,x}} \; ; \; \Delta t \leq \frac{\Delta y}{c_{g,y}} \qquad (3.2.1)$$

In the SWAN model the balance action equation is integrated by implicit numerical schemes, by the finite differences method in time and in the geographical and spectral space.

The time is discretized, with a time interval Δt constant, to integrate both the terms, the wave propagation and the initial terms $S(\sigma, \theta)$.

The geographical space is described by a rectangle defined by grid cells of dimensions Δx and Δy constant in the directions *x* and *y,* respectively.

3.2.1 Spread in the geographical and spectral space

The numerical scheme used by SWAN solves the partial derivates present in the equations of the spreading process in the frequency and direction space, by the method of finite differences.

Through experiments with the 2nd generation HISWA model (Holthuijsen et al., 1989), it was noted that for coastal zones, models based on spectral balance equation can be associated with the spread in the geographical space (Holthuijsen, 2007).

$$\frac{\partial c_{g,y} N(\sigma,\theta)}{\partial y} \simeq \left[\frac{\left[c_y N\right]_{i_y} - \left[c_y N\right]_{i_y-1}}{\Delta y} \right]_{t+1} \qquad (3.2.1.1)$$

$$\frac{\partial c_{g,x} N(\sigma,\theta)}{\partial x} \simeq \left[\frac{\left[c_x N\right]_{i_x} - \left[c_x N\right]_{i_x-1}}{\Delta x} \right]_{t+1} \qquad (3.2.1.2)$$

When using the scheme above, the directional space is decomposed into four quadrants at each point of the geographical space. The calculations are performed in each quadrant irrespective of the other, with the exception of energy action that moves across borders between the quadrants. The transfer of energy or action that occurs between the components of the waves from different directions is thus taken into account iteratively. After completion of the four phases, the energy of the wave is propagated in the total geographic domain.

As in the spread in the geographical space, the Courant Fredrik-Levy (CFL) condition also applies to the spectral space. The CFL parameter should not exceed the unit, in order to follow a stability criteria in the numerical approximations made. The accuracy of the results, as mentioned, is also one of the criteria that a numerical scheme must satisfy.

The SWAN model uses exclusively a first order numerical scheme for regressive differences spread in the geographical space. In the spectral space the situation is different since the spread in this space requires greater accuracy. Because of that it is adopted a combination between a second order difference scheme, more economical in terms of time spent in the calculations, then a first order scheme of regressive differences.

$$\frac{\partial c_\sigma N(\sigma,\theta)}{\partial \sigma} \simeq \left[\frac{(1+\mu)(c_\sigma N)_{i_\sigma+1} - 2\mu(c_\sigma N)_{i_\sigma} - (1-\mu)(c_\sigma N)_{i_\sigma-1}}{2\Delta\sigma} \right]_{t+1} \qquad (3.2.1.3)$$

$$\frac{\partial c_\theta N(\sigma,\theta)}{\partial \theta} \simeq \left[\frac{(1+\upsilon)(c_\theta N)_{i_\theta+1} - 2\upsilon(c_\theta N)_{i_\theta} - (1-\upsilon)(c_\theta N)_{i_\theta-1}}{2\Delta\theta} \right]^{n+1} \quad (3.2.1.4)$$

The SWAN model presents three alternatives in the numerical scheme choice to use for the process of wave propagation in geographic and spectral space.

They are: first-order difference scheme delayed, BSBT-"Backward Space, Backward Time" — applied to stationary or non-stationary conditions; second-order scheme S&L (Stelling and Leendertse, 1992), used for stationary conditions; second-order scheme SORDUP – *"Second Order, UPwind"* - (Rogers et al., 2002), used for stationary conditions.

3.2.2 Generation, dissipation and nonlinear wave interactions

The parameter *A* described in the spectral energy balance equation, relative to the linear growth of wave energy, does not depend on the shape of the spectrum and therefore it can be directly integrated by the values of the wind characteristics, speed and direction.

All remaining terms, responsible for the wave energy transfer, are dependent on the energy density and can be described by $S = \phi E$, where ϕ is a coefficient obtained from the integral parameters of the waves.

The SWAN integrates the initial terms, i.e., wave generation by wind and non-linear interactions between three and four positive waves, in order to achieve a more stable model. The scheme then is described by the term in the source level *n* and by iterating to the previous level of energy density E^{n-1}.

$$S^n \approx \phi^{n-1} E^{n-1} \quad (3.2.2.1)$$

Contrary to the positive contributions, the partial shoaling, bottom friction, shoaling induced by the bottom and nonlinear interactions between three and

four waves when negative, require an implicit scheme in order to obtain a stable model.

The shoaling induced by decreased depth is represented by a linear phenomenon, which is estimated at level *n* of the iteration, with a linear approximation of the previous level *n* −1.

$$S^n \approx \phi^{n-1} E^n + \left(\frac{\partial S}{\partial E} \right)^{n-1} (E^n - E^{n-1}) \tag{3.2.2.2}$$

The remaining negative terms, where the nonlinear effects are weakest, the partial shoaling, the bottom friction and the non-linear interactions between three and four waves, are integrated in a similar way:

$$S^n \approx \phi^{n-1} E^{n-1} + \left(\frac{S}{E} \right)^{n-1} (E^n - E^{n-1}) \tag{3.2.2.3}$$

With $S = \phi E$, the expression is reduce to:

$$S^n \approx \phi^{n-1} E^n \tag{3.2.2.4}$$

3.3 Limitations

SWAN brought several positive impacts for wave studies and marine forecasts, however, as with any other model, there are limitations that researchers and stakeholders need to be aware. Among the limitations of the model is the need to calibrate many of the parameters involved in the description of the different physical phenomena, which it was based on data from JONSWAP campaign, conducted in the North Sea.

Such parameters may not be correct for areas with different characteristics of wave climate associated with the state of sea, wave and curl or to different characteristics of the seabed.

Diffraction at the SWAN is modeled simply as a directional dispersion, which may constitute its main limitation, and does not consider the effects of Bragg scattering.

The inclusion of diffraction in numerical calculations implies that the spacing of the computational grid, in relation to the wavelength, is such that guarantee the convergence of computer calculations. This implies sometimes that the grid dimensions are of such size that can derail the implementation of the calculations.

SWAN does not compute the currents induced by the waves. If relevant, the currents must be provided as an input data to SWAN.

The LTA approximation for the triad wave-wave interactions depends on the width of the directional distribution of the wave spectrum. The present tuning in SWAN seems to work reasonably in many cases but it has been obtained from observations in general conditions.

The DIA approximation for the quadruplet wave-wave interactions depends on the width of the directional distribution of the wave spectrum. It seems to work reasonably in many cases, but it is a poor approximation for long-crested waves (narrow directional distribution). It also depends on the frequency resolution. It seems to work reasonably in many cases, but it is a poor approximation for frequency resolutions with ratios very different from 10%. This is a fundamental problem that SWAN shares with other third-generation wave models, such as WAM and WAVEWATCH III.

SWAN can be used on any scale relevant for wind generated surface gravity waves. However, SWAN is specifically designed for coastal applications that should actually not require such flexibility in scale. The reasons for providing SWAN with such flexibility are to allow this model to be used from laboratory conditions to shelf seas and to nest SWAN in the WAM model or the WAVEWATCH III model which are formulated in terms of spherical coordinates.

Nevertheless, these facilities are not meant to support the use of SWAN on oceanic scales, because SWAN is less efficient on oceanic scales than WAVEWATCH III and probably also less efficient than WAM.

4 CASE STUDY RESEARCH NAZARÉ CANYON

4.1 Characterization

Nazaré is a Portuguese village, located in the west central part of Portugal with about 10300 inhabitants. Throughout the 20th century, Nazaré progressively evolved from a fishing village to a village dedicated to tourism, having been one of the first international tourist interest points in Portugal. The tourism industry is today one of the major employers in the village and the Nazaré canyon drives the increase in visitors during the season of giant waves.

There are two mainly beaches at Nazaré, the Northern and the Nazaré beaches (Figure 4.1). The Northern beach is located at the vicinity of the Nazaré submarine Canyon and is presently being studied in the scope of several research projects. This coastal stretch exhibits a particular behavior with the interaction of wave and currents with the complex morphology of the Nazaré canyon head.

Figure 4.1: Northern and Nazaré beaches location. Font: Google earth 2014.

Among a dozen canyons in the Portuguese continental margin, the Nazaré canyon is undoubtedly one of the most imposing. In addition to being one of the largest in the world, it rips off the continental shelf, perpendicular to the coast, and extends for more than 210 Km from the abyssal depths of 5000 m until a few meters from the coast (Figure 4.2).

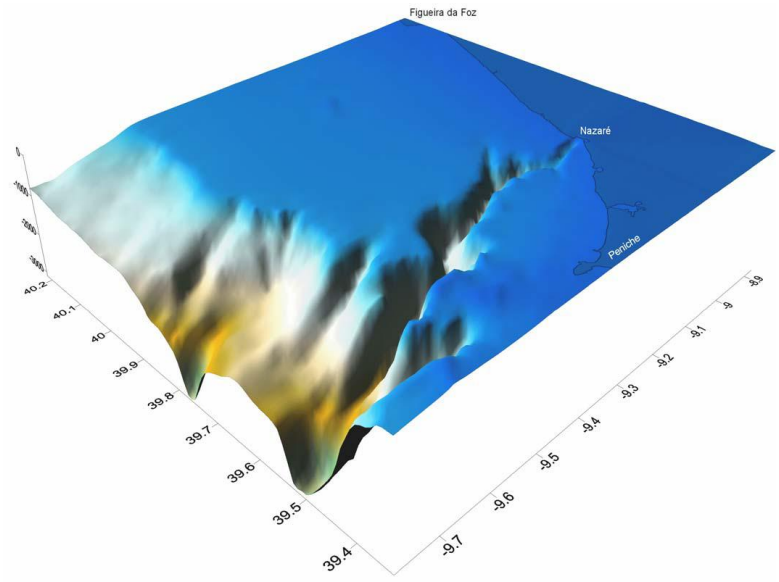

Figure 4.2: Nazaré ´s bathymetry – Font: Portuguese Hydrographic Institute.

Being a huge topographic feature, the Nazaré canyon plays an important role in regional water masses circulation (Vitorino et al., 2005). Its characteristics favor mass and energy transit between the internal platform regions and the deep ocean. The canyon axle configuration promotes the convergence of baroclinic energy and the divergence of barotropic energy (Quaresma 2000).

As a consequence, there is the spread of a large-amplitude internal tide along its internal domain (Quaresma et al., 2000), as well as a reduction in the amplitude of the tide along the coast of Nazaré (Sauvaget et al., 2000).

The Nazaré canyon presents the characteristics of a “gouf” canyon, due to its large dimensions, the longitudinal slope down (between 10 to 20%) with the head deeply carved into the coastline (Shepard & Drill, 1966; Vanney & Mougenot, 1981; 1990).

The main thalweg has a general orientation Est-West and a "V" shape. The main axis is consists of 4 sections, joined by rectilinear abrupt curves, accented by the presence of several ravines(Vanney & Mougenot, 1981).

The main tributary is the Vitoria tributary, NE-SW orientation, connected to the main thalweg (North Bank) near the bathymetric of 600 m. The South face is more complex, intersected by numerous small tributaries, sometimes installed in fracture zones.

In this sector of the canyon occurs numerous sedimentary and hydrodynamic phenomena, responsible for its erosive nature and, therefore, by its deep notch on the coast.

4.2 Giant waves

The oceans cover about 2/3 of the Earth's surface and the giant waves are not that rare, all that is needed is a sufficiently powerful ocean storm and series of such storms happen each year.

The location is a key factor in this complex process. Giant waves that do not travel far enough away from their source storms will remain with chaotic shapes. When a giant wave approaches the coast, the contour of the seafloor is what controls the final size and shape of the wave before it reaches the coast. Finally, the local wind determines the final quality of the waves.

Nazaré is a "beach break" and there is a drastic change in the seafloor that amplify the waves, but there are other factors and processes that in combination, significantly increase the wave height, which can achieve heights much higher than the values registered offshore.

These processes and factors are described and represented in the Figure 4.3.

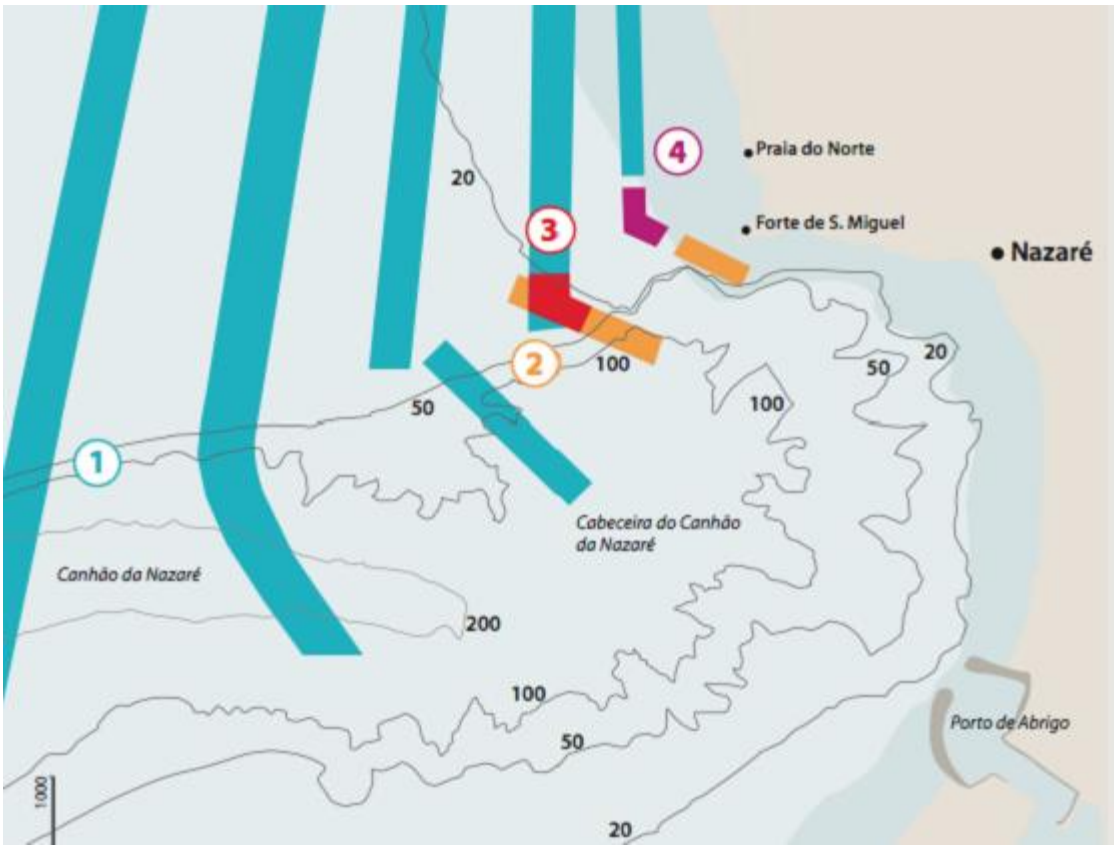

Figure 4.3: Shoaling of the wave approaching Northern beach. 1-Wave refraction, 2- Wave shoaling, 3-Sum of two waves, 4- Local drift – Font: Portuguese Hydrographic Institute.

With the arrival of a strong swell in the Portuguese coast with waves coming from the West/Northwest quadrants, it is possible to note in the point **1** the wave refraction, which occurs because of the depth differences between the continental shelf and the canyon. This effect change the wave direction on the canyon, where the wave travels faster. In the point **2** it´s verified an overtopping of the topographic step (vertical gap from the bottom). The depth reduction originates wave shoaling (reduction of its wavelength and the amplification of its height). This effect also occurs gradually with the wave approaching to the coast. In the point **3** is noted the positive interference between the wave on the canyon and the wave that crosses the Northern continental shelf. This effect promotes new shoaling at the intersection point of these two waves. In the section **4**, where is originated the local drift, the waves promotes a current along the beach that flows from North to South. This current intersects the wave in the opposite direction of its spread. This process contributes additionally to the shoaling of the wave.

Because of these process and factors the wave height can achieve

height much higher than the values registered offshore, as occurred in October 2013, when the Brazilian surfer Carlos Burle surfed a supposed 30 meters wave (Figure 4.4).

Figure 4.4: Carlos Burle on a supposed 30 m wave in Nazaré – Photo: Tó Mané.

5 SWAN APPLICATION

Through the simulations done with the SWAN model it is possible to analyze the Nazaré canyon influence at the wave regime in the region. To start the simulations it´s necessary to provide a file with the model bathymetry data and an input file that defines all the parameters of the model configuration (annex).

These parameters are related to the boundary conditions, the definition of geographic, temporal and spectral domain, physical phenomena's to considerate in the calculations, and the kind of output data in order to numerically integrate the action balance equation.

On the side borders, perpendicular to the shoreline, when there is no conditions introduced the spectral density is considered null in adjacent areas. By imposing these side conditions, the results will always have some mistakes in the wave propagation through the computational area.

The affected area depends on the sea conditions, and on the area defined by the directional wave energy distribution width. In a situation of wind sea the angle is typically 30 °, while for the swell will vary between 5º and 10º (SWAN Team, 2008) (Figure 5.1).

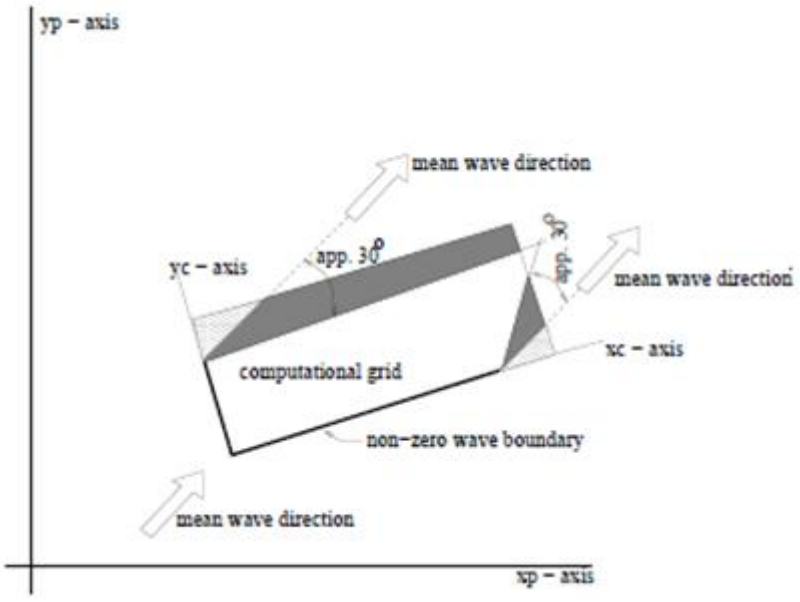

Figure 5.1: Disturbed regions in the computational grid due to erroneous boundary conditions are indicated with shaded areas. SWAN Team (2008).

Regardless of the boundary type, the model assumes that all the wave energy which "get out" of the computational domain is lost. The energy which "comes" in the field, usually make part of a boundary parallel to the shoreline, which is necessarily provided by the user.

It is possible, on SWAN model, to introduce the maritime agitation as boundary conditions in parametric or spectral shape. In the first case, which was adopted for this work, it is necessary to provide the values of significant height, peak or average length, the average direction for the peak frequency and the dispersion direction. In the second case the boundary conditions provided to the SWAN are specified by:

- A bidimensional discrete spectrum $E(\sigma, \theta)$;
- A discrete one-dimensional spectrum $E(\sigma)$followed by the mean and dispersion direction for each frequency;
- An empirical uni-dimensional spectrum with a directional empirical distribution

As a third alternative, the SWAN presents three scenarios for the spectrum imposition: JONSWAP spectrum, the Pierson-Moskowitz spectrum and the spectrum of Gaussian shape (Ris, 1997).

The model also allows the choice between the nautical or cartesian convention for the input and output data and to the waves direction and wind. The nautical convention defines a system of axes relative to the geographic north, the wind and waves direction are measured in a clockwise direction. In the cartesian convention measurements are made in the opposite direction of clockwise (Figure 5.2).

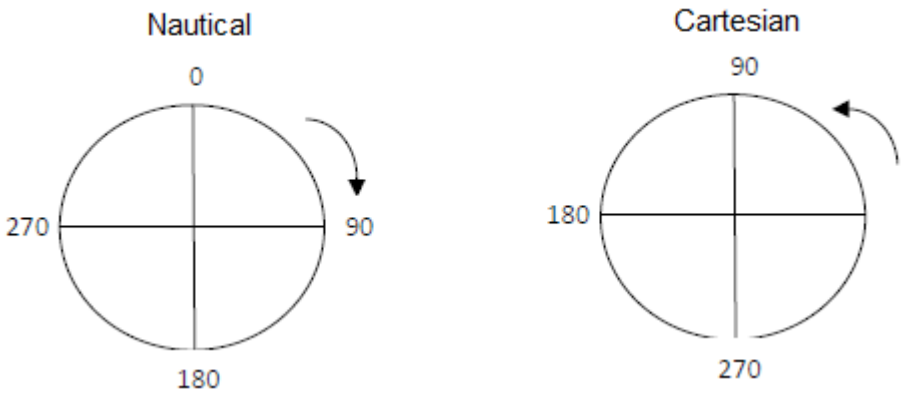

Figure 5.2: Representation of Nautical and Cartesian conventions respectively.

The SWAN allows defining the geographical location of the area under study, such as its size and its resolution, and even the choice between a system of nautical or cartesian coordinates. In the cartesian system, the geographical origin (0,0) of all domains is set by the user, and their locations are defined relative to a certain "local coordinate system" (Figure 5.3).

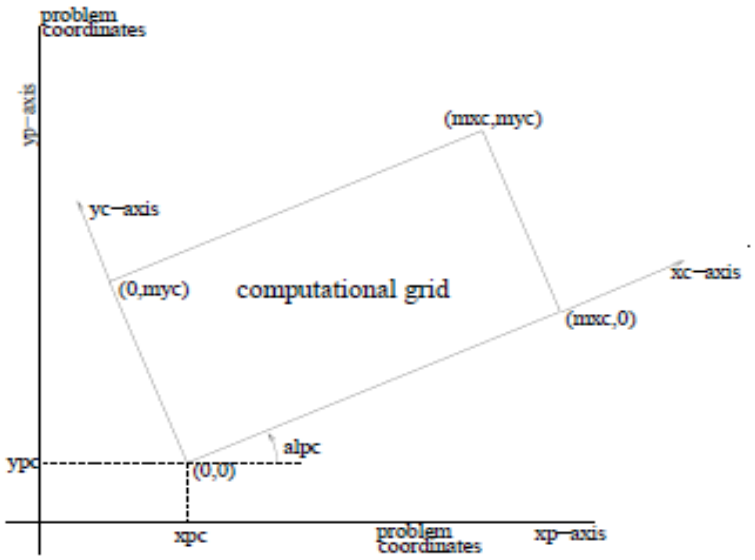

Figure 5.3: Coordinates Xpc and Ypc corresponding to the origin of the calculation domain, relative to the "local coordinate system". Adaptation of an image by SWAN Team (2008).

For a large domain the SWAN model allows performing multiple runs embedded, that is, the definition of areas coupled with different resolutions and

dimensions to obtain a more realistic description of the wave propagation parameters.

In directional space, SWAN realize all calculations of the wave´s components coming from the range of directions that the user imposes.

The SWAN model allows to include different physical phenomena that can affect the wave´s propagation. For example the refraction, shoaling, bottom friction, partial breaking and induced decrease in depth, the nonlinear interaction of three and four waves and the interaction with the currents in the form of refractive shoaling and frequency variation.

The output can be controlled by the user defining their locations and types for parametric or spectral shape.

5.1 Numerical implementation

The numerical implementation was done in a Cartesian coordinates system through two regular meshes with different resolutions system. The bathymetry was provided by the Hydrographic Institute. This bathymetry consisted on soundings with irregular spacing in the order of 360 m. It was constructed a regular grid with quadrangular units in the same order of magnitude as the original, and a subsequent grid defined by a resolution four times smaller than the previous one, in the order of 90 m. This grid was constructed with a better resolution to provide more realistic results.

The wave´s propagation in coastal areas is influenced by bathymetry and to get a true representation of its effects, it is necessary to increase the spatial resolution toward the coast. All the grids were defined in military rectangular coordinates relative to Lisboa Datum (source system local coordinates).

It was adopted a kind of coupling that involved two grids (Figure 5.4). The first grid has a greater domain source X_{01}=56 638 and Y_{01}=242 835 and has a length of 100 080 m perpendicular to the shoreline and 100 080 m parallel to this, with a resolution of 360 m. The second grid originates X_{02}=*96 059* e Y_{02}=*268 284* and has dimensions of 34 560 m perpendicular to the shoreline and 42 840 m parallel to this, with a resolution of 90m.

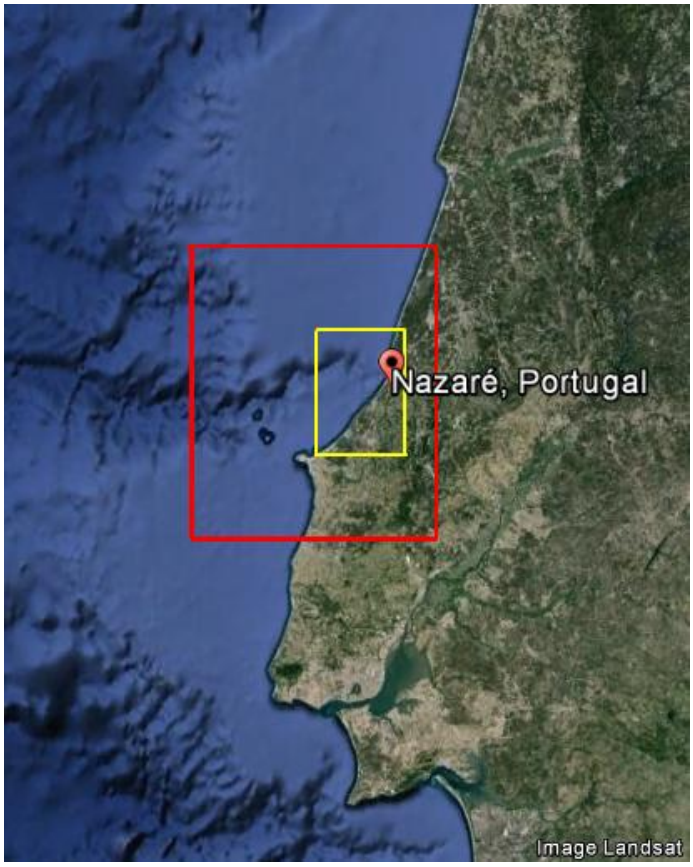

Figure 5.4: Computational domains used in SWAN.

Although the grids have been coupled, the calculations are extended to the entire area of each grid. Initially, the model proceeds to the calculations in the first grid and the results of this are used as boundary condition in the second, running up the SWAN again to determine the wave propagation in the adjacent area to Nazaré beach. The accuracy of the results is greater when resorting to the nested grid system, among other reasons, by no longer be relevant the boundary conditions in the lateral zones of the larger domain (Pires Silva et al., 2002) .

5.2 Simulations

In order to verify the influence of the Nazaré canyon in the characteristics of the wave regime in the region, the SWAN model implementation developed

was tested under different conditions and a sensitivity analysis was performed for different cases.

Considering that the boundary conditions waves are introduced parametrically, it is necessary to provide the values of significant wave height, average or peak period of the wave, the average direction for the peak frequency of the wave and the dispersion direction.

In this analysis, a simulation is done using the actual bathymetry of the study area, with the Nazaré canyon. The waves direction in simulations were considered from Northwest and from West. For the height and the wave period, values ranging from 1 m to 30 m of significant height with periods of 8, 12 and 16 s (Table 5.1) were adopted.

These boundary conditions values were chosen because they are frequently registered during the different seasons in the region.

Table 5.1: Variations in the parameters used in simulations.

Direction (Dir^{o})	Wave height (m)	Period (s)
West	1	8 -12 -16
	2	8 -12 -16
	3	8 -12 -16
	4	8 -12 -16
	5	8 -12 -16
	6	8 -12 -16
	7	8 -12 -16
	8	8 -12 -16
	9	8 -12 -16
	10	8 -12 -16
	15	8 -12 -16
	20	8 -12 -16
	30	8 -12 -16
North West	1	8 -12 -16
	2	8 -12 -16
	3	8 -12 -16
	4	8 -12 -16
	5	8 -12 -16
	6	8 -12 -16
	7	8 -12 -16
	8	8 -12 -16
	9	8 -12 -16
	10	8 -12 -16
	15	8 -12 -16
	20	8 -12 -16
	30	8 -12 -16

In a synthetic scenario, a simulation is made with a modified bathymetry without the Nazaré canyon, being the parameter values and the boundary conditions the same used in the first scenario. This change in bathymetry was done through a specific tool for treating bathymetry of the MOHID modeling system and consisted of changing the seafloor, so that the Nazaré canyon was no longer noticeable. (Figure 5.5).

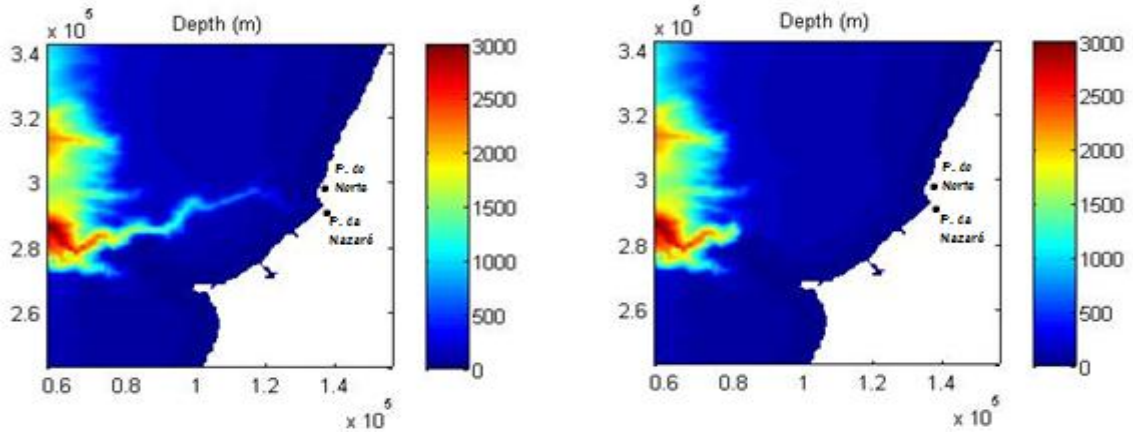

Figure 5.5: Bathymetry on the largest grid – with the canyon and without the canyon.

For a better comprehension of the wave regime in the Nazaré coastal region, the analysis was elaborated from the simulations with the smaller grid (Figure 5.6), which has a better resolution.

Maps representing the simulations results were elaborated through dedicated MATLAB subroutines.

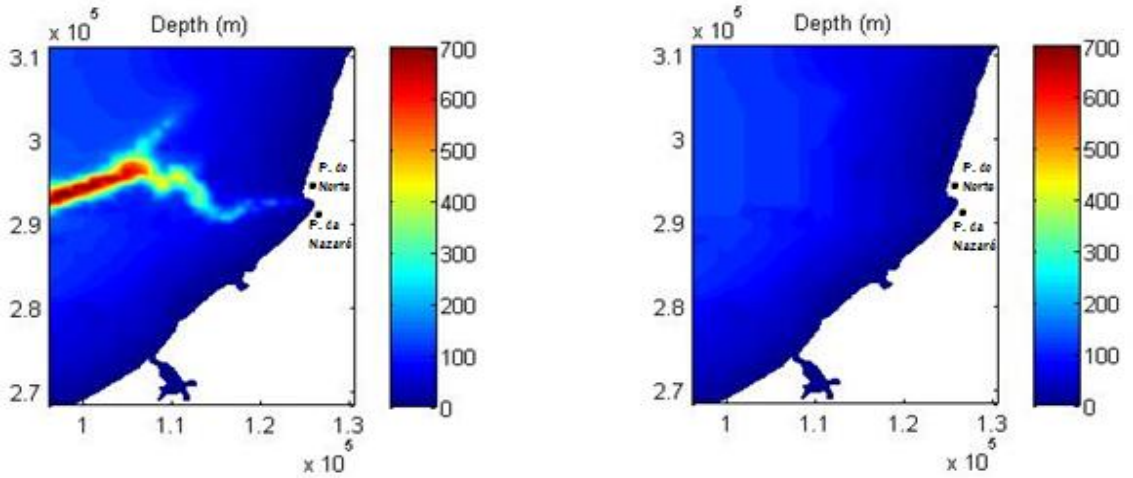

Figure 5.6: Bathymetry on the smaller grid – with the canyon and without the canyon.

The following results were analyzed:

- Wave Height, H_{sig} (*m*)
- Wave Direction, Dir (º)
- Wave Period, P (*s*)
- Wave Length, Wlen (*m*)
- Orbital Velocity, Ubot (*m/s*)

6 RESULTS

The simulations were performed with various different combinations of forcing conditions, considering several directions, height and wave period data (Table 5.1). As a result of the simulations, several maps were generated. Among these, it were selected those who had a better representation of the Nazaré canyon influence in the wave regime of this region.

In a first analysis, the forcing conditions that were used correspond to values of a situation already observed in the Nazaré region, with waves coming from the West, with heights of 1 m and periods of 12 s, and a second scenario, with values relating to largest sea waves coming from the Northwest, with heights of 5 m and longer periods of 16 s.

These second scenario parameters are values calculated in a storm day (Figure 6.1), in which the Brazilian surfer Carlos Burle surfed maybe the largest wave ever surfed in history, approximately 30 meters.

Portugal - **Nazaré**, Lat: **39.6**, Lon: **-9.075**

GFS 50 km	Ondulação (m)								Direcção da vaga								Periodo da vaga (s)							
	00h	03h	06h	09h	12h	15h	18h	21h	00h	03h	06h	09h	12h	15h	18h	21h	00h	03h	06h	09h	12h	15h	18h	21h
26.10.2013	3.2	3.1	3	2.8	2.6	2.5	2.3	2.2	↘	↘	↘	↘	↘	↘	↘	↘	13	13	13	12	12	11	11	11
27.10.2013	2	1.9	1.8	1.7	2.1	3.4	5	5.7	↘	↘	↘	↘	↘	↘	↘	↘	11	10	10	10	17	21	20	19
28.10.2013	5.6	5.3	4.9	4.8	4.6	4.5	4.5	4.4	↘	↘	↘	↘	↘	↘	↘	↘	19	18	18	17	16	16	15	14
29.10.2013	4.4	4.3	4.2	4	3.8	3.6	3.5	3.4	↘	↘	↘	↘	↘	↘	↘	↘	14	14	13	13	13	13	13	12
30.10.2013	3.2	3.1	2.9	2.7	2.6	2.4	2.2	2	↘	↘	↘	↘	↓	↘	↘	↓	12	12	12	12	12	11	11	11

Figure 6.1 : Wave height, direction and period in a storm day. Font: © 2000 - 2014 www.windguru.cz.

The maps are subdivided into: with Nazaré canyon, on the left side and without Nazaré canyon on the right. At the bottom, the images were enlarged for a better understanding of the waves development along the coast.

6.1 Waves height

The first analysis considers the influence of the Nazaré canyon in the waves height at the study area.

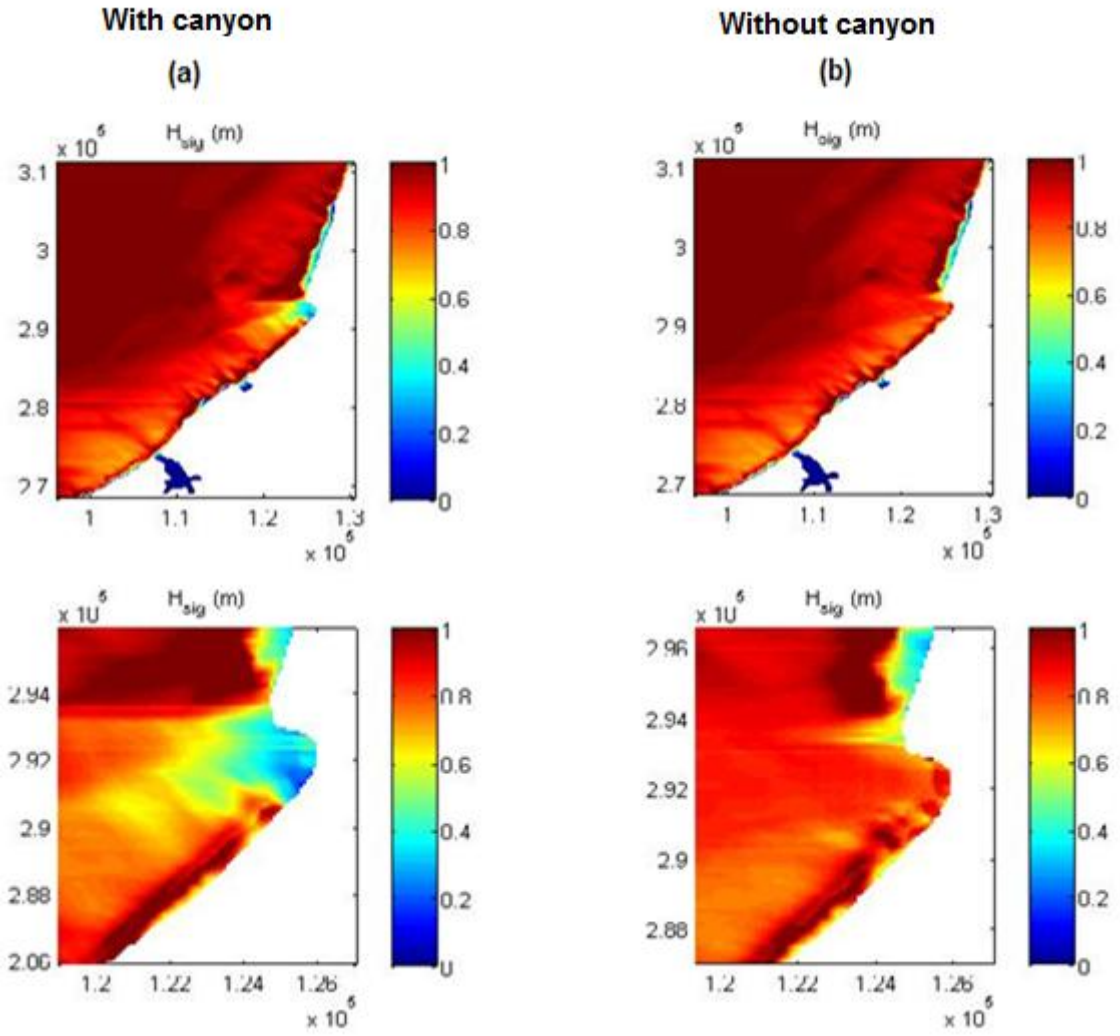

Figure 6.2: Predicted significant height with waves coming from the West, with 1 m height and 12 s period. Scenario (a) with canyon and scenario (b) without canyon. Below are the enlarged images.

In this first simulation (Figure 6.2), is observed that in a real scenario (a), in the largest view, the wave maintains a pattern size along the northern coast, reaching the equivalent of 0.4 m height. This pattern is markedly altered in significant height as the waves approach to the head of the canyon, where the waves hit the Northern beach with approximately 1 m height, which is equivalent to the forcing imposed. This means that the wave decreases slightly in height when it slides over the canyon.

It´s possible to notice also the position where the wave refraction occurs due to the difference in depths between the continental shelf and the canyon. From this position the wave travels faster over the canyon after changing

direction, when occurs a reduction in the wavelength and amplification of its height (shoaling) .

Following the coast line, it is verified that the height of the waves hitting the Nazaré beach has a reduced value between 0 m and 0.4 m. This is because the canyon "change" the direction of the wave towards Northern beach.

In the synthetic scenario (b) without the Nazaré canyon, the waves maintains a standard size along the northern coast, reaching the same heights equivalent to 0.4 m. When approaching the bedside of the canyon, there is a decrease in wave height near the Northern beach. On this occasion the waves vary around 0.4 m and 0.6 m in height.

In this scenario, since there are already no topographic difference between the canyon and the continental shelf, at the head of the canyon, the waves have a significant height almost constant, gradually decreasing to the coast of the Northern beach

A very interesting point in this analysis is the influence that the Nazaré canyon makes in Nazaré beach. In the simulation without the canyon, the waves sometimes reach heights between 0.8 m and 1 m at this point of the coast, validating the idea that the canyon deflect the waves into the Northern beach.

By changing the direction, height and wave period of boundary conditions, respectively, for Northwest, 5 m and 16 s, the wave height maps were generated from simulations (Figure 6.3).

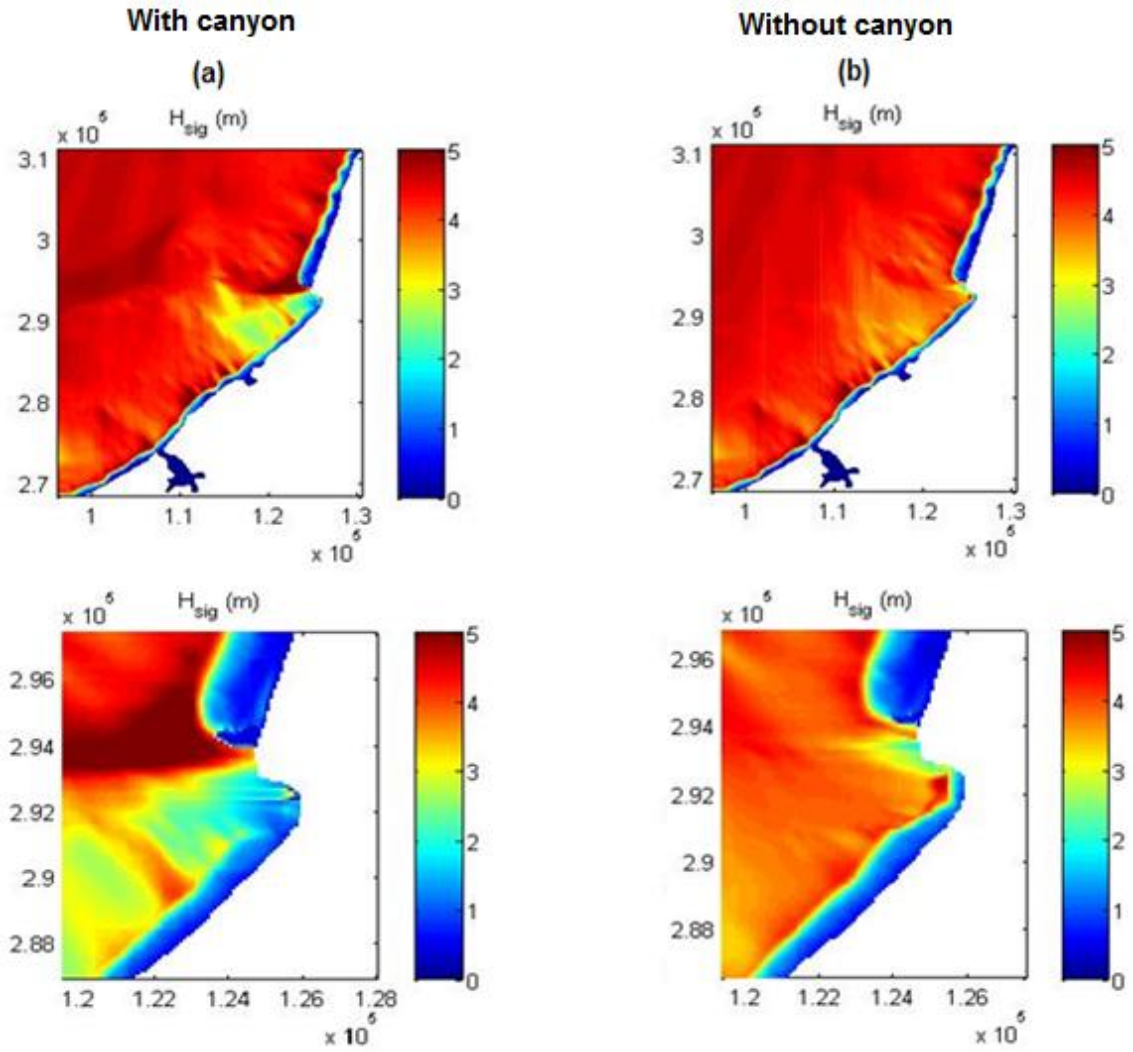

Figure 6.3: Predicted significant height with waves coming from Northwest, with 5 m in height and a 16 s period. Scenario (a) with the canyon and scenario (b) without the canyon. Below are the enlarged images.

In the scenario with the real bathymetry (a), it´s possible to verify that along the Northern beach, big waves dissipate before reach the coast. Approaching the canyon´s head, it is noted that in a certain area along the valley, there is a height value of approximately 1 m below the 5 m imposed as a forcing. This pattern occurs because in this area is originated the local drift, where there is current flowing along the beach from North to South. This current flows in the same direction and intersects the wave propagation in the opposite direction. This process contributes effectively to the shoaling of the wave.

As emphasized in the first simulation presented, in this second simulation, with waves coming from Northwest, 5 m height and long periods of 16 s it still possible to notice the wave height difference over the canyon, due to

the declivity of the shelf. In this case, the waves hit the shore at the beginning of the Northern beach with heights of up to 5 m.

The mathematical model SWAN is not able to simulate the actual height of the waves at this point. As mentioned in the previous chapter, the SWAN does not calculate sum of two waves, which is exactly what happens in this point, where two waves with different speeds and directions are added, forming large waves.

In the South of the cabe, Nazaré beach is "protected" again from the big swells that are induced towards the Northern beach.

In the synthetic scenario (b) without the Nazaré canyon, waves maintains the same standard size along the northern coast, showing that the absence of the canyon does not have great influence in the area.

Approaching to the canyon´s head, it turns out that in the same area along the valley, in the northern part, where it originates local drift, the value of height of about 1 m is still present, but covers a smaller area than when the canyon is considered.

Since there are no topographic difference between the canyon and the continental shelf, at the head of the canyon, the waves have a nearly constant height of approximately 4 m, reaching the Northern beach coast with this value.

In Nazaré beach, south of the cape, was again observed an increase in wave height due to absence of the Nazaré canyon

.

6.2 Waves direction

In the following situation, the parameter under analysis is the wave direction, Dir (º). The same values of direction, height and period used in previous simulations were kept.

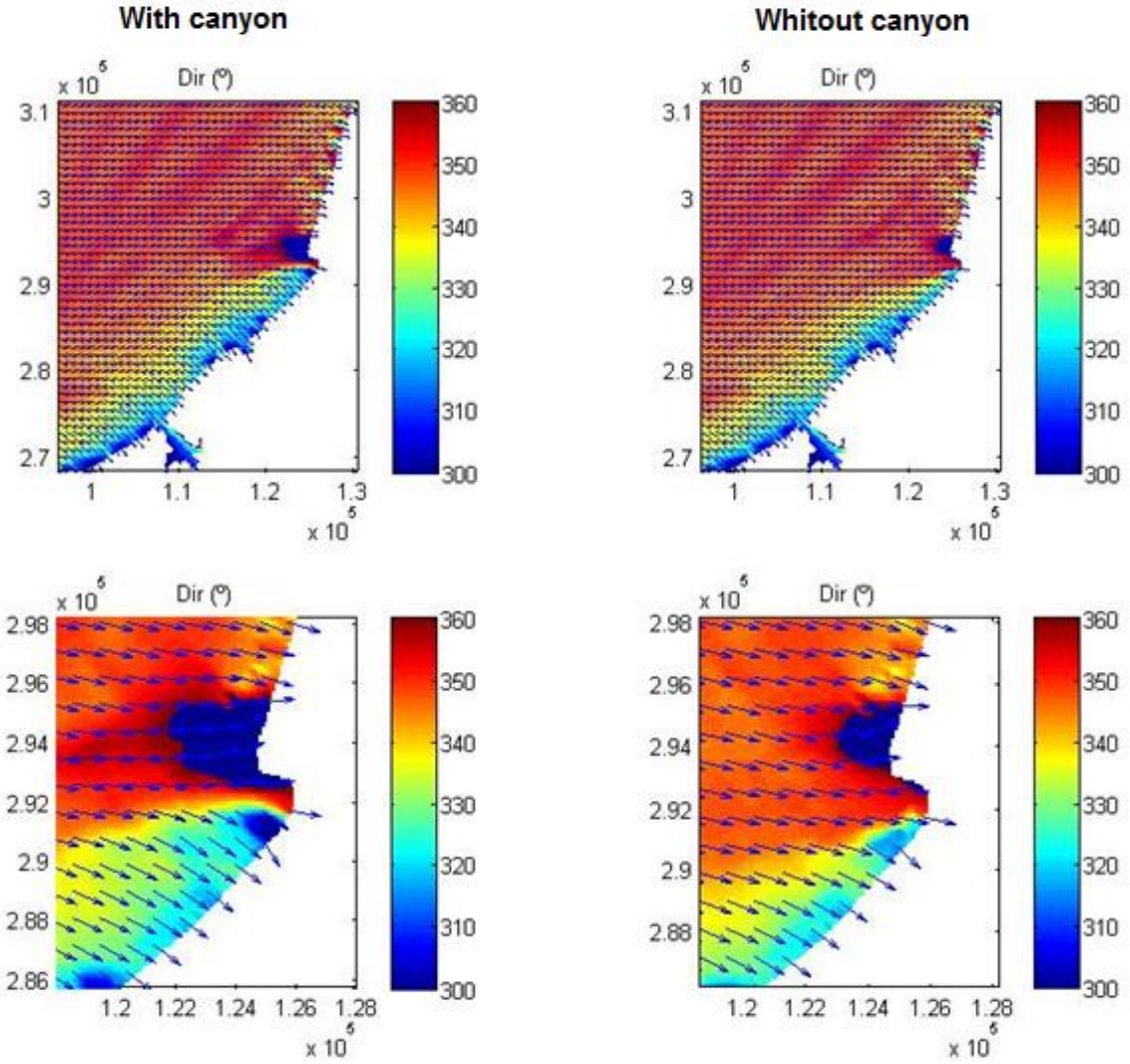

Figure 6.4: Predicted directions with waves coming from the West, with 1 m in height and a 12 s period. Scenario with canyon and without canyon. Below are the enlarged images.

In a simulation with waves coming from West, 1 m height and 12 s period (Figure 6.4), in a real scenario of the region's northernmost cape the waves run along the coast perpendicularly to the direction previously set, hitting the coast with directions ranging from West and Northwest.

When spreading on the canyon, the wave maintains the same West direction, until the moment they reach the declivity between the canyon and the continental shelf, where the refraction occurs. At that moment the waves increase in speed and reach the coast with a Southwest direction.

The Nazaré beach receives waves with alternately directions. In a location near to the cape, the waves reached the coast in the West / Southwest

direction. More to the south, the waves have West directions. Following the coastline it is possible to observe that the waves take the Northwest direction.

In the situation where the canyon is not present, almost nothing changes in the northern region of the study area, thus verifying that the absence of the canyon has no big influence in this area. The largest change of direction is exactly where was the canyon, and also in the Southern part.

When approaching the coast, the wave undergoes a new change of direction, as in the first simulation, reaching the coast with waves coming from West / Southwest, but in a smaller area.

At the Nazaré beach, the absence of the Canyon implies a higher incidence of waves coming from West / Northwest, and along the south coast it is noted that the canyon does not cause big changes regarding the directions.

In a simulation with waves coming from the Northwest with 5 m height and 16 s period, were generated the maps represented in Figure 6.5.

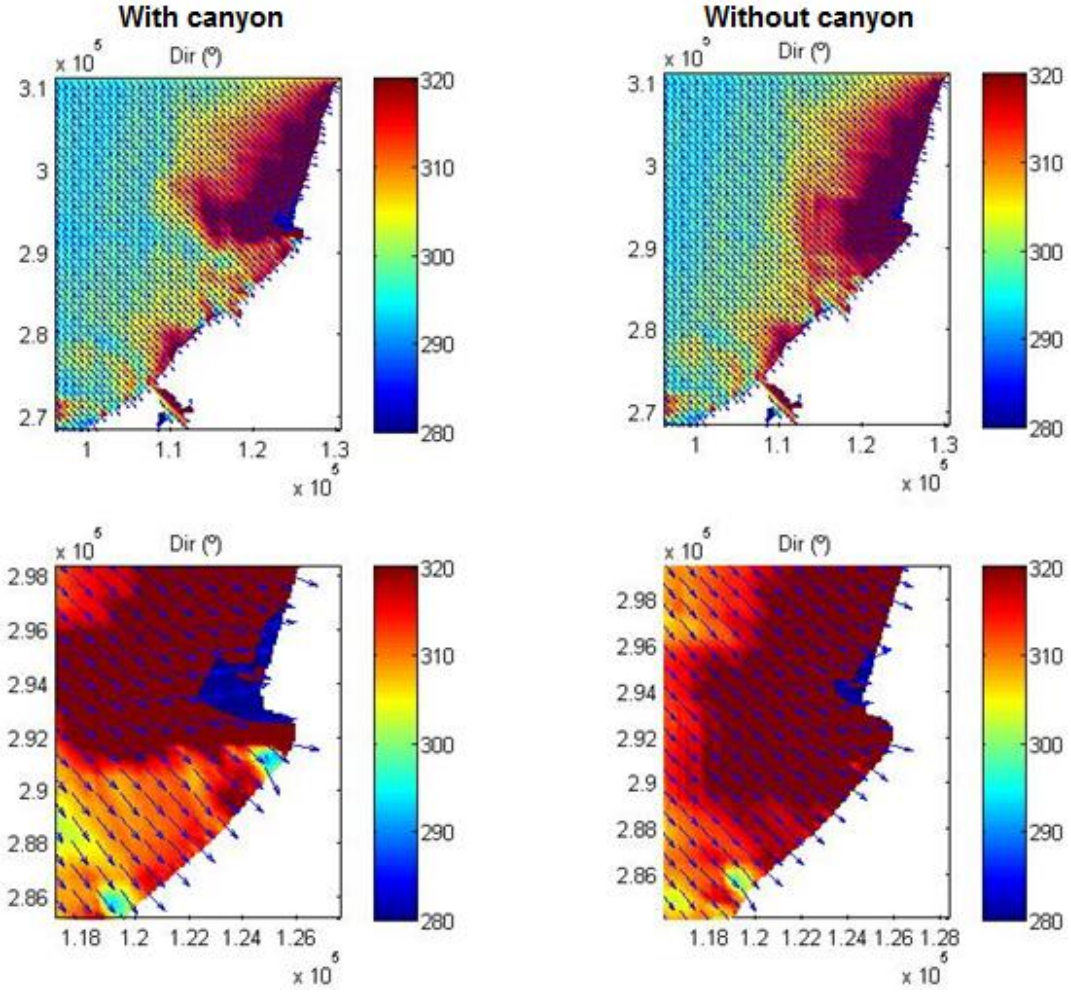

Figure 6.5: Predicted directions of waves coming from the Northwest, with 5 m in height and a 16 s period. Scenario with canyon and without canyon. Below are the enlarged images.

The large waves with long periods coming from the Northwest, when arriving on the canyon, are deviated to the West, reaching perpendicularly the North beach.

It´s possible to notice that in the absence of the canyon, the largest change in the waves direction is just at the south of the large submarine valley, where the waves vary Northwest to the West/Northwest.

6.3 Waves period

The simulation performed to identify the influence of the Nazaré canyon in the period of the waves was done with waves coming from the West, 1 m height and 12 s period (Figure 6.6)

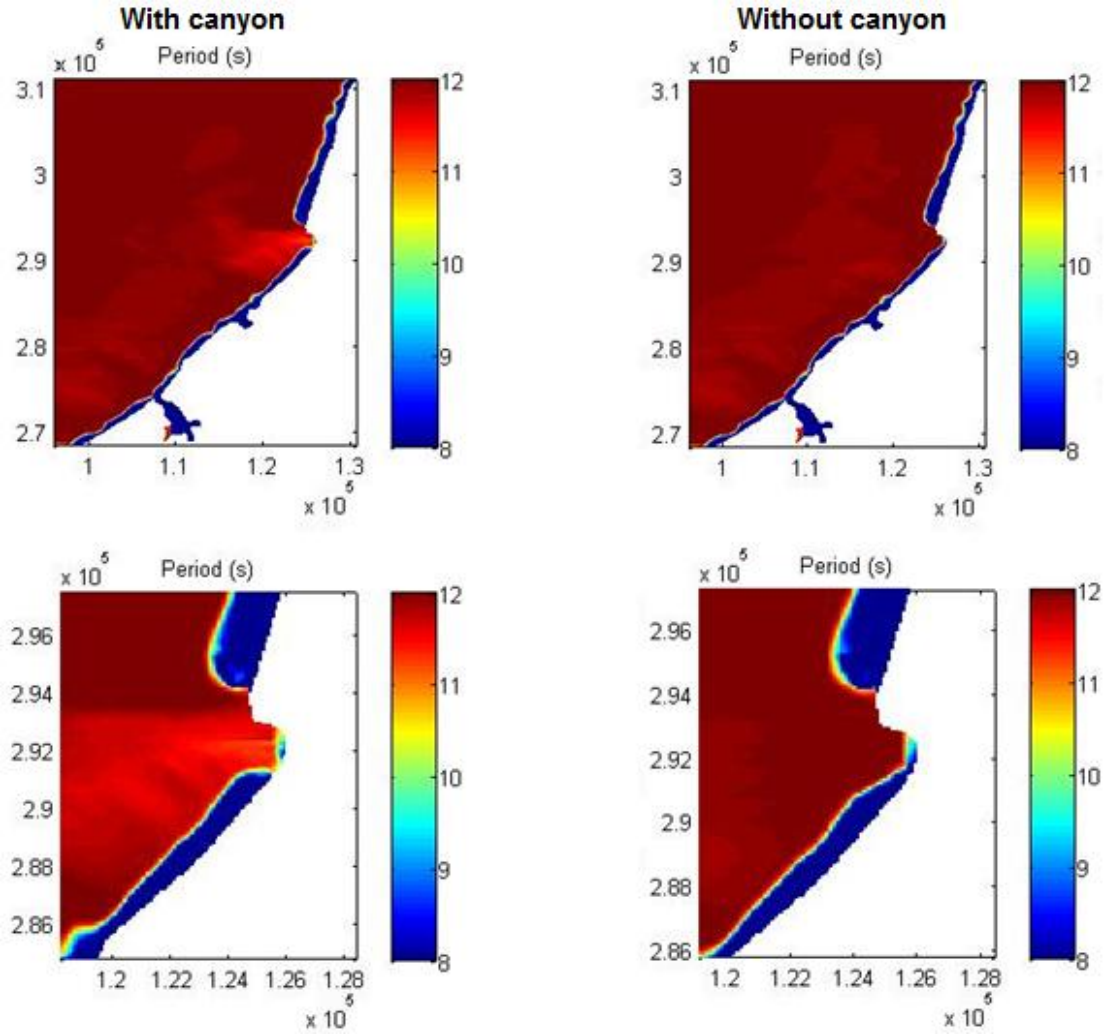

Figure 6.6 : Predicted periods with waves coming from the West, with 1 m in height and a 12 s period. Scenario with canyon and without canyon. Below are the enlarged images.

The period of a wave is defined as the time it takes two successive crests to pass a fixed point. Since the period of 12 seconds was initially imposed, it appears that this value is maintained until the moment that the waves pass by the topographic difference generated by the canyon. At this moment refraction occurs, the waves slide on the canyon in the same 12 s period, but just in the south this value decreases approximately 1s.

In the scenario without the canyon, the difference of periods over the canyon and its adjacent area disappears. The period of the waves decreases gradually finding lowest depths.

6.4 Wavelength

In respect to wavelength, the simulations with the waves coming from Northwest, with 5 m high and 16 s period (Figure 6.7) showed the largest change.

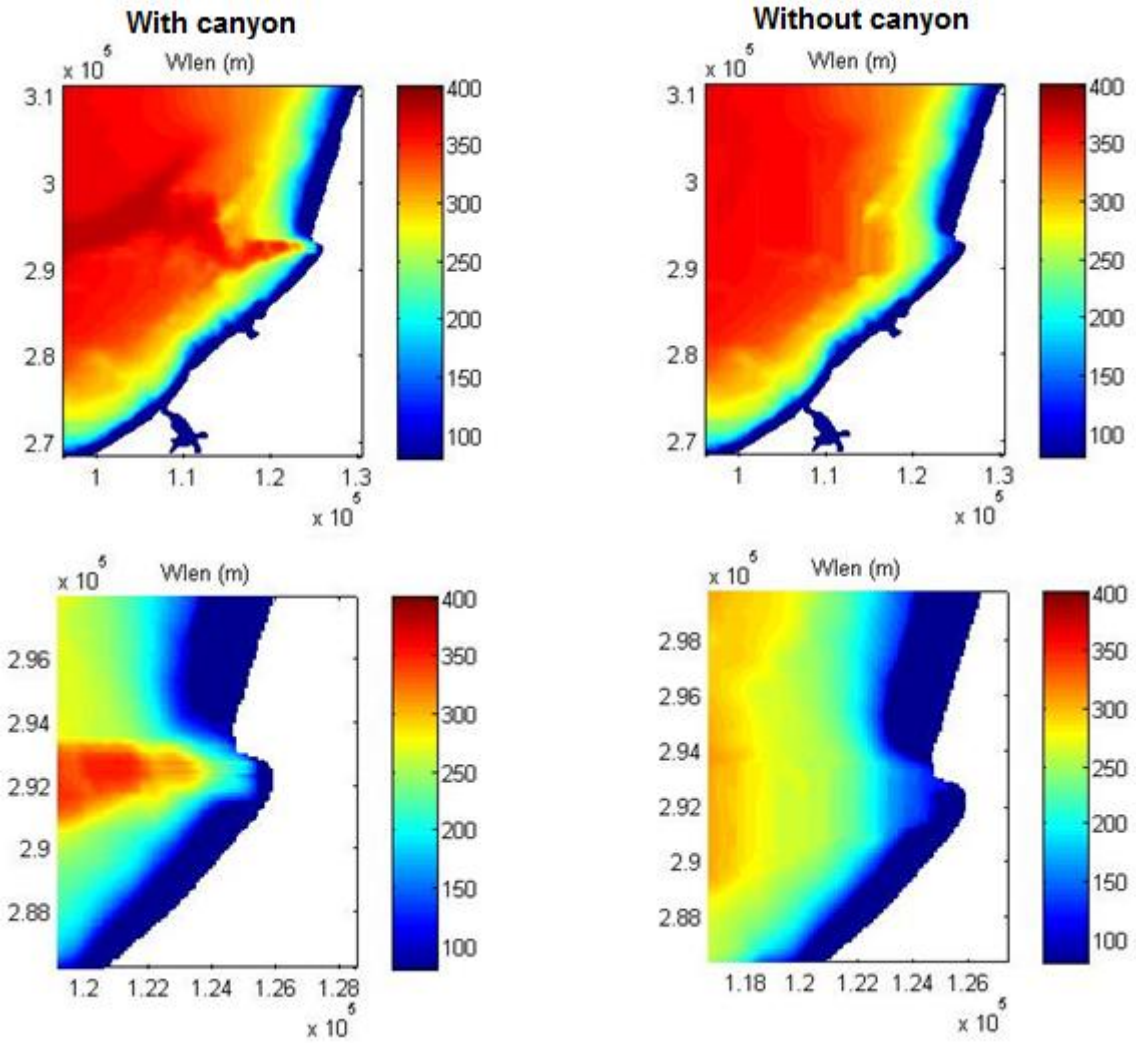

Figure 6.7 : Predicted wavelength with waves coming from the Northwest, with 5 m in height and a 16 s period. Scenario with canyon and without canyon. Below are the enlarged images.

When the period is a very high, it is known that the wavelength tends also to be high. In the case of this simulation, the waves reached 400 m in length over the canyon. However the waves begin to reduce in length as they approach the shoaling area, reaching wavelengths between 200 m and 300 m.

6.5 Orbital velocity

In respect to the orbital velocity, the simulations that represented a interesting change of scenario were the simulations with waves coming from Northwest, with 5 m height and 16s period.

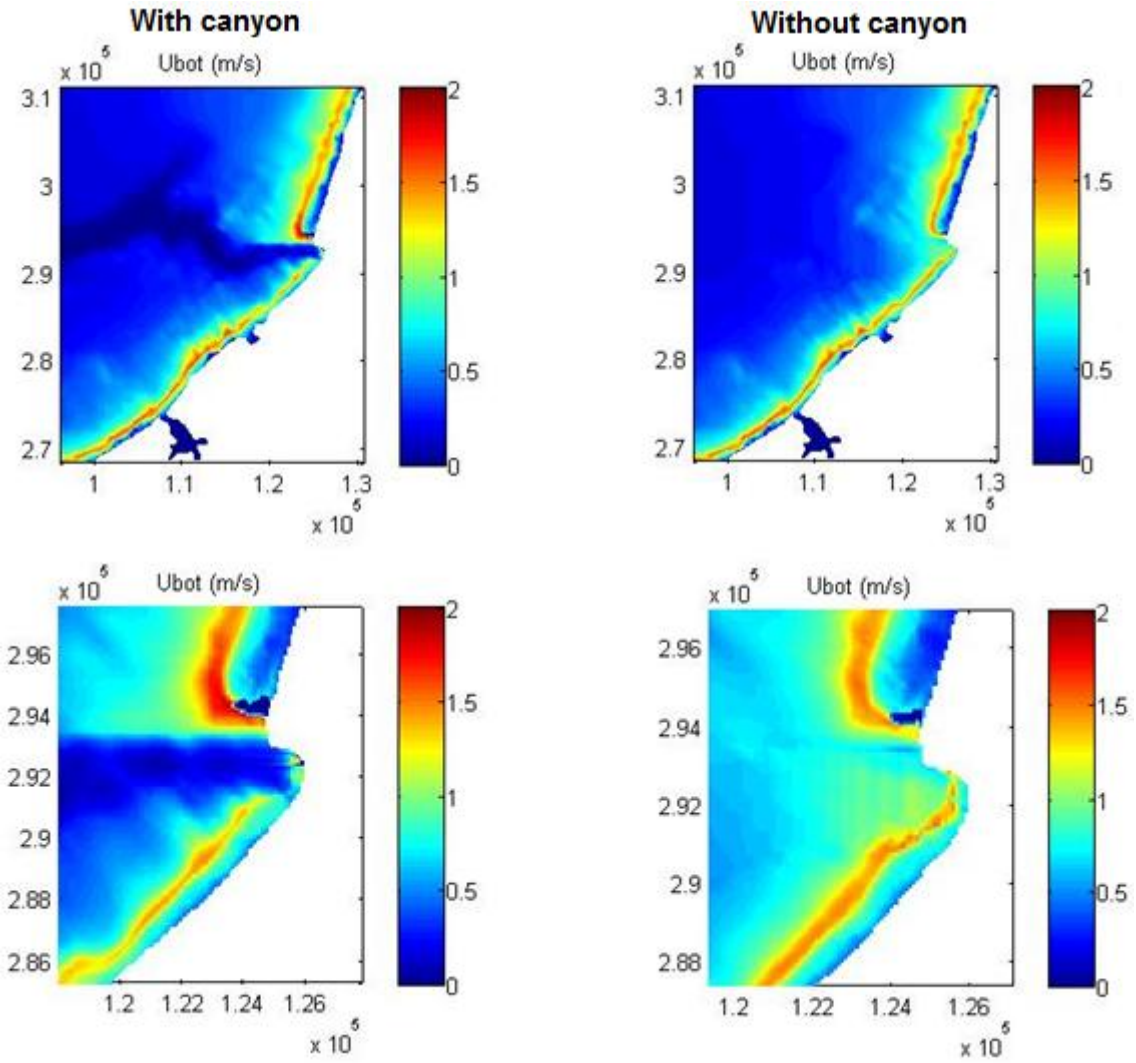

Figure 6.8 : Predicted orbital velocity with waves coming from Northwest, with 5 m in height and a 16 s period. Scenario with canyon and without canyon. Below are the enlarged images.

Analyzing Figure 6.8, it´s possible to notice that in the scenario with the canyon, the orbital velocity is practically zero in the valley. However, in the synthetic scenario without the canyon, the orbital velocity follows a pattern with approximately 1 m/s velocity.

In the enlarged image, it is noted that in the first scenario, the area where it is originated the local drift, with the orbital speed almost 0 m/s, covers a larger space than it covers in the map without the canyon. The orbital speed reaches approximately 2 m/s in the region where the wave shoaling occurs, while in the scenario without the canyon, in that point the orbital speed reach approximately 1.5 m/s.

6.6 Wave height dependence on forcing conditions

To understand if there is a relation between the waves that reached the Northern and Nazaré beaches and the forced waves height, two graphics were elaborated. Simulations were performed in the scenarios with and without canyon with West waves direction, ranging from 1 m to 10 m height with 16 s period (Table 6.1).

Table 6.1: Height values of forced wave compared with values of wave height that where obtained as response in Northern and Nazaré beaches.

	With Canyon		**Without Canyon**	
Height imposed (m)	Northern beach (m)	Nazaré beach (m)	Northern beach (m)	Nazaré beach (m)
1	0.9	0.1	0.9	0.8
2	1.8	0.4	1.6	1.5
3	2.6	0.5	2	2.3
4	3.9	0.8	2.2	2.8
5	4.6	1	2.3	3.1
6	4.8	1.2	2.4	3.8
7	4.9	1.5	2.3	3.8
8	5	1.8	2.4	3.8
9	5.2	2.2	2.3	3.8
10	5.3	2.3	2.2	4

In the computational grid two different points were chosen, one on the Northern beach and another in the Nazaré beach. The wave significant height from these points were compared with the wave significant height imposed. (Figure 6.9, 6.10 and Table 6.1).

Analyzing the graphics it's possible to observe a considerable difference between the waves significant height in scenarios with and without canyon in both beaches. That is because there is no more topographic difference between the canyon and the continental shelf and the waves do not suffer refraction and follow the direction initially imposed.

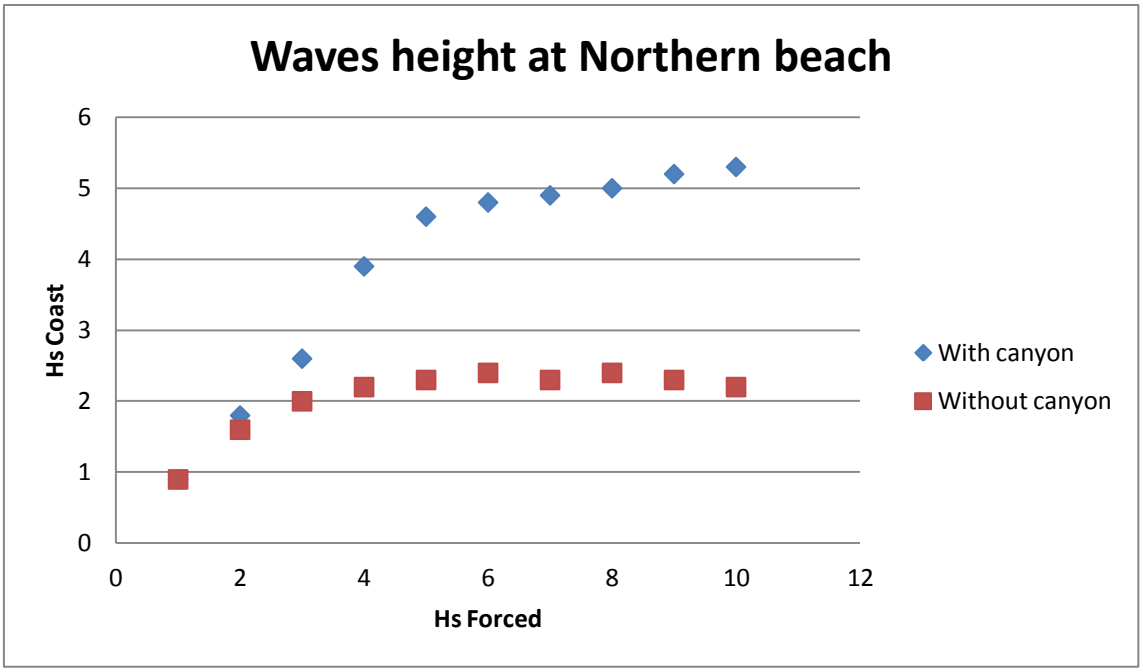

Figure 6.9 : Waves height at Northern beach.

In simulations on the Northern beach with the canyon, it is observed that there is a linearity between the Northern beach wave height with the height imposed, however this linearity is interrupted when the imposed waves exceed 5 m, in this moment the waves at the Northern beach maintain the height of approximately 5 m. In the scenario without the Nazaré canyon, it´s noted that the waves has a remarkable decrease in height when they reach the Northern beach. When the waves imposed reach between 4 m and 10 m height, the waves at the Northern beach do not exceed 2.5 m height.

The effect of the canyon at the Northern beach is that the waves tend to be larger on the Northern beach with the canyon then without the canyon.

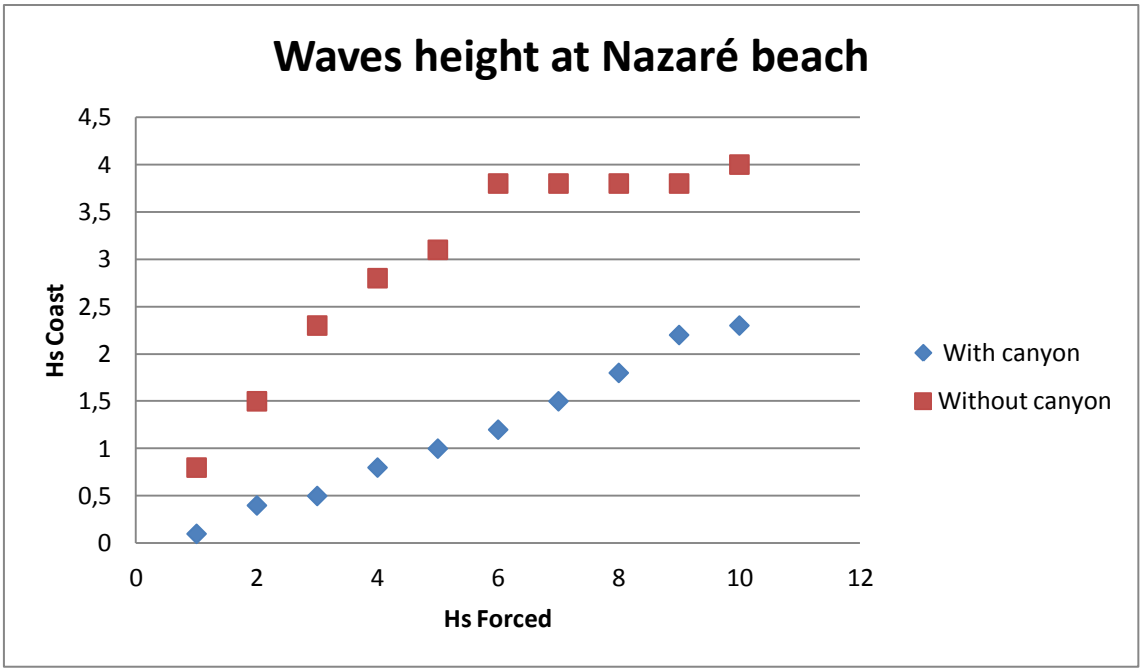

Figure 6.10 : Waves height at Nazaré beach.

However on the Nazaré beach it is noted that the waves height does not follow the waves heights imposed, because as was mentioned in another review, the Nazaré canyon change the wave direction to the Northern beach. In the scenario with the canyon the waves maintain an increase pattern in proportion to the imposed waves and they does not exceed 2.5 m height. In the scenario without the canyon is observed a significant change in the waves height on the Nazaré beach, the waves are higher than in Northern beach, but the largest waves does not exceed 4 m in height

The effect of the canyon at the Nazaré beach is the opposite that happen in Northern beach, the waves tend to be largest without the canyon because the waves do not suffer refraction and follow the direction initially imposed.

7 CONCLUSION

The present work had as main objective the implementation of SWAN model in a real scenario with a bathymetry courtesy of Hydrographic Institute (IH) and in another scenario, with a synthetic bathymetry without the Nazaré canyon.

The model was used in stationary state. This means forcing the simulations without the wind variable fields and impose in a parametric form the boundary conditions.

By using the stationary state, it is not necessary to resort to a calculation domain with large dimension, and this implies a low number of points calculation, and consequently also low computation times. This circumstance allowed to run SWAN model for several different simulations, which facilitated a better analysis of the influence of the Nazaré canyon in the wave regime.

Regarding the mathematical model SWAN, it´s possible to conclude that it represents an important tool in predicting the characteristics of wave propagation in any coastal area, and can be inserted in projects of risk assessment of erosion and flooding in coastal areas or alert systems against storms and very rough seas for shipping or in harbor areas.

Whatever the application, it is important to note that the simulations performed with the SWAN model depend on the parameters and conditions of application of this model. It also has some limitations, specifically in the case of Nazaré, where the SWAN does not show the actual height of the waves because they are a sum of two waves traveling at different speeds.

The results of the simulations performed by SWAN along the Nazaré coast, in different scenarios, with and without canyon, confirm the importance of the Nazaré canyon in the wave regime in this region. In general, all parameters had specific changes, but the changes of direction, height and orbital velocity of the waves, are the ones that showed differences that would cause a largest changing on the wave regime in the region.

In a scenario without the canyon, it was possible to conclude that the waves which were previously diverted to the Northern beach, head towards Nazaré beach. These waves also suffer an increase in height in the south of the cape.

This study indicate that the absence of the Nazaré canyon would indisputable change the wave regime in the area. The effect of the canyon at the Northern beach is that the waves tend to be larger on the Northern beach with the canyon then without the canyon. The effect of the canyon at the Nazaré beach is the opposite that happen in Northern beach, the waves tend to be largest without the canyon because the waves do not suffer refraction and follow the direction initially imposed.

7.1 Future works

Regarding to the results obtained with the SWAN mathematical model used in this study, it was created an expectative in how does the model could work with a more refined grid, with a more extensive dataset, which could further improve the results. Another proposal for future work is to apply the mathematical model SWAN in the creation of artificial reefs in a region, with the aim of improving the conditions of waves surfed, which would result in a greater demand from surfers around the world, increasing the tourist activity and consequently the economy of the region.

REFERENCIAS

Airy, G. B. (1841). Hugh James Rose, et al., ed. "Encyclopædia Metropolitana". Mixed Sciences 3 (published 1817–1845).

Battjes,J.A.,1994, Shallow water wave modeling, *Proc.Int. Symp.: Waves – Physical and Numerical Modeling*, eds. M. Isaacson and M.Quick, Vancouver, University of British Columbia, I,pp. 1-23.

Booij, N., R.C. Ris and L.H. Holthuijsen, 1999, A third-generation wave model for coastal regions, Part I, Model description and validation, *J.Geoph.Research*, 104, C4, 7649-7666.

Booij, N., Haagsma, I.J.G., Holthuijsen, L.H., Kieftenburg, A.T.M.M., Ris, R.C., van der Westhuysen, A.J., Zijlema, M., 2004. User Manual for SWAN, Version 40.41. Delft University of Technology, Delft, The Netherlands.

Eldeberky, Y., 1996: Nonlinear transformation of wave spectra in the nearshore zone, *Ph.D. thesis*, Delft University of Technology, Department of Civil Engineering, The Netherlands

Fenton, J.D., 1985. A fifth-order Stokes theory for steady waves. ASCE. J. Waterw. Port Coast. Ocean Eng. 111, 216–234.

Hasselmann, K. and 15 authors (1973): Measurements of wind wave growth and swell decay during the Joint North Sea Wave Project (JONSWAP). Dt. Hydrogr. Z., A8(12), 95 pp.

Holthuijsen, L.H. Booji, Herbers, T.H.C., 1989, A prediction model for stationary, short crested waves in shallow waters with ambient currents, *Coastal Engineering*, **13**, 23-54.

Holthuijsen, Leo H., 2007, *Waves in Oceanic and Coastal Waters*, Cambridge University Press

Komen, G.J., Cavaleri, L., Donelan, M., Hasselmann, K., Hasselmann, S. and P.A.E.M. Janssen, 1994: *Dynamics and Modelling of Ocean Waves*, Cambridge University Press, 532 p.
Miles, J. W. (1957): On the generation of surface waves by shear flow. J. Fluid Mech., 3, 185–204.

Phillips, O. M. (1958): The equilibrium range in the spectrum of wind-generated ocean waves. J. Fluid Mech., 4, 426-434.

Pires Silva, A.A., Makarynskyy, O., Monbaliu, J., Ventura Soares, C. e Coelho, E.(2000), Modelling wave transformation in an open beach on the west coast of Portugal, *Proc.COASTAL WAVE MEETING*, A. Sanchez-Arcilla, S.Ponce de Leon (Eds.) Technical Universityof Catalonia, Barcelona,.4.3.

Pires Silva, A.A., Makarynskyy, O., Monbaliu, J., Ventura Soares, C. e Coelho, E.(2002), Wam/Swan Simulations in an Open Coast: Comparisons with ADCP Measurements, *Littoral 2002, The Changing Coast.* EUROCOAST/EUCC, Porto – Portugal.

Quaresma, L. S., 2000. Estudos Em Oceanografia Física - Maré Interna no Canhão Submarino da Nazaré. B.Sc Thesis, Évora University, Portugal.

Quaresma, L. S., Coelho, E. F., Rosa, L., Beja, J., 2000. Internal tide on Nazaré submarine canyon – head canyon measurements. *Proceedings of 3rd Symposium on the Iberian Atlantic Continental Margin*, Faro, Portugal, 165-166.

Quaresma, L. S., 2006. Observação de ondas internas não lineares geradas sobre o canhão submarino de Nazaré. Thesis, Lisboa University, Portugal.

Ribeiro, M. S. A., 2008. Dinâmica sedimentar no canhão da Nazaré. Faculdade de Ciências da Universidade de Lisboa. Portugal.

Ris, R. C., 1997: Spectral modeling of wind waves in coastal areas. Ph.D. thesis, Delft University of Technology, 160 pp.

Rogers, W.E., J.M. Kaihatu, H.A. H. Petit, N. Booij, and L.H. Holthuijsen, 2002: Diffusion reduction in a arbitrary scale third generation wind wave model, *Ocean Engineering*.1357-1390.

Sauvaget, P., David, E., Guedes Soares, C., 2000. Modelling tidal currents on the coast of Portugal. Coastal Engineering, 40, 393-409.

Shepard, F. & Drill, R. (1966) – Submarine canyons and other sea valleys. Rand McNally, Chicago, 381pp.

Smith G.D. (1978), *Numerical solution of partial differential equations*, Oxford University Press, Walton Street, Oxford.

Stelling, G.S. and J. J. Leendertse, 1992, Approximation of convective processes by cyclic AOI methods, *Proc.2nd Int. Conf. Estuarine and Coastal Modeling* (Tampa), New York, ASCE, pp.771-782

Stewart, R.H., 2002. Introduction to Physical Oceanography. Texas A & M University, Cap.16.

Stokes, G. G. (1847). "On the theory of oscillatory waves". *Transactions of the Cambridge Philosophical Society* 8: 441–455. Reprinted in: Stokes, G. G. (1880). *Mathematical and Physical Papers, Volume I*. Cambridge University Press. pp. 197–229.

SWAN team: Booij, N., Haagsma, I.J.G., Holthuijsen, L.H., Kieftenburg, A.T.M.M., Ris, R.C., van der Westhuysen, A.J., Zijlema, M., 2008. SWAN, Technical Documentation, Cycle III, version 40.51. Delft University of Technology, Delft, The Netherlands.

Vanney, J. & Mougenot, D. (1981) – La plate-forme continentale du Portugal et les provinces adjacentes: Analyse Geomorphologique. Mem. Serv. Geol. Portugal, 28: 145 pp.

Vanney, J. & Mougenot, D. (1990) – Un canyon sous-marin du type “gouf”: le Canhão da Nazaré (Portugal). Oceanologica Acta, 13 : pp. 13 – 14.

Vitorino, J., Oliveira, A., Beja, J., 2005. The Nazare Canyon (W Portugal): Physical processes and sedimentary impacts. *Geophysical Research Abstracts*, EGU2005, 7, 10013.

WAMDI: Hasselmann, S., Hasselmann, K., Bauer, E., Janssen, P.A.E.M., Komen, G.J., Bertotti, L., Lionello, P., Guillaume, A., Cardone, V.C., Greenwood, J.A., Reistad, M., Zambresky, L., and Ewing, J.A., 1988. The WAM model – A Third Generation Ocean Wave Prediction Model, J. Phys. Ocean., vol. 18, 177 p.

ANNEX

Input file to the exterior domain

```
PROJECT 'grid1   ' '1'

$********MODEL INPUTS*********
SET level=0

CGRID  56638.21    242835.74    0.00 100080. 100080.   277 277 SECTOR -180.00  120.00 30
.050 .200  15

INPGRID BOTTOM REGULAR   56638.21    242835.74  0.00  277 277  360. 360.
READINP BOTTOM 1. 'grid1.bot   ' 3 0 FREE

$********BOUNDARY CONDITIONS*********
BOUN SHAP GAUSS PEAK DSPR POWer
BOUN SIDE S  CCW CONSTANT PAR       10.00     16.00    -15.00   4.00
BOUN SIDE N  CCW CONSTANT PAR       10.00     16.00    -15.00   4.00
BOUN SIDE W  CCW CONSTANT PAR       10.00     16.00    -15.00   4.00

$********PHYSICS**********************
OFF WINDGROWTH
OFF WCAPPING
OFF QUAD
TRIAD
FRICTION MADSEN               7.9999998E-02

$********NUMERICAL REQUESTS**********
NUMERIC ACCUR .05 .05 .05 95.00 STAT 20

$********OUTPUT REQUESTS**************
NGRID 'border'  96059.46    268284.36   0.00  34560. 42840.  383 475
NESTOUT 'border' 'nest4grid2.nst'
FRAME   'border2'  56638.21    242835.74   0.00  100080. 100080.   277 277
TABLE 'border2' HEADER 'output.dat' XP YP DEPTH HS PER DIR WLEN FORCE UBOT
COMPUTE
HOTFILE 'hotstart_grid1.hst  '
STOP
```

Input file of nested mesh

```
PROJECT 'grid2   ' '1'

$********MODEL INPUTS*********
 SET level=0

 CGRID  96059.46    268284.36   0.00  34560. 42840.  383  475 SECTOR -180.00  120.00 30
.050 .200  15

 INPGRID BOTTOM REGULAR  96059.46    268284.36  0.00  383 475   90.  90.
 READINP BOTTOM 1. 'grid2.bot   ' 3 0 FREE

$********BOUNDARY CONDITIONS*********
 BOUND NEST 'nest4grid2.nst      '

$********PHYSICS**********************
 OFF WINDGROWTH
 OFF WCAPPING
 OFF QUAD
 TRIAD
 FRICTION MADSEN              7.9999998E-02

$********NUMERICAL REQUESTS**********
 NUMERIC ACCUR .05 .05 .05 95.00 STAT 20

$********OUTPUT REQUESTS**************
 NGRID 'border'  96059.46    268284.36   0.00   34560. 42840.  383  475
 NESTOUT 'border' 'nest4grid3.nst'
 FRAME   'border2'  96059.46    268284.36   0.00   34560. 42840.  383  475
 TABLE 'border2' HEADER 'output1.dat' XP YP DEPTH HS PER DIR WLEN FORCE UBOT
 COMPUTE
 HOTFILE 'hotstart_grid1.hst  '
 STOP
```

Input file to the interior domain

```
PROJECT 'grid1   ' '1'

$********MODEL INPUTS*********
 SET level=0

 CGRID  56638.21    242835.74    0.00 100080. 100080.  277 277 SECTOR -180.00  120.00 30
.050 .200  15

 INPGRID BOTTOM REGULAR   56638.21    242835.74  0.00  277 277  360. 360.
 READINP BOTTOM 1. 'grid1.bot   ' 3 0 FREE

$********BOUNDARY CONDITIONS*********
 BOUN SHAP GAUSS PEAK DSPR POWer
 BOUN SIDE S  CCW CONSTANT PAR        10.00      16.00    -15.00   4.00
 BOUN SIDE N  CCW CONSTANT PAR        10.00      16.00    -15.00   4.00
 BOUN SIDE W  CCW CONSTANT PAR        10.00      16.00    -15.00   4.00

$********PHYSICS**********************
 OFF WINDGROWTH
 OFF WCAPPING
 OFF QUAD
 TRIAD
 FRICTION MADSEN               7.9999998E-02

$********NUMERICAL REQUESTS**********
 NUMERIC ACCUR .05 .05 .05 95.00 STAT 20

$********OUTPUT REQUESTS**************
 NGRID 'border'  96059.46    268284.36    0.00  34560. 42840.  383 475
 NESTOUT 'border' 'nest4grid2.nst'
 FRAME   'border2'  56638.21    242835.74   0.00  100080. 100080.   277 277
 TABLE 'border2' HEADER 'output.dat' XP YP DEPTH HS PER DIR WLEN FORCE UBOT
 COMPUTE
 HOTFILE 'hotstart_grid1.hst  '
 STOP
```

Input file of nested mesh

```
PROJECT 'grid2   ' '2'

$********MODEL INPUTS*********
 SET level=0

 CGRID  96059.46     268284.36    0.00 34560. 42840.  383 475 SECTOR -180.00  120.00 30
.050 .200  15

 INPGRID BOTTOM REGULAR   96059.46    268284.36  0.00 383 475  90.  90.
 READINP BOTTOM 1. 'grid2.bot   ' 3 0 FREE

$********BOUNDARY CONDITIONS*********
 BOUND NEST 'nest4grid2.nst      '

$********PHYSICS**********************
 OFF WINDGROWTH
 OFF WCAPPING
 OFF QUAD
 TRIAD
 FRICTION MADSEN               7.9999998E-02

$********NUMERICAL REQUESTS**********
 NUMERIC ACCUR .05 .05 .05 95.00 STAT 20

$********OUTPUT REQUESTS**************
 NGRID 'border'  96059.46    268284.36   0.00   34560. 42840.  383 475
 NESTOUT 'border' 'nest4grid3.nst'
 FRAME   'border2'  96059.46    268284.36   0.00   34560. 42840.  383 475
 TABLE 'border2' HEADER 'output1.dat' XP YP DEPTH HS PER DIR WLEN FORCE UBOT
 COMPUTE
 HOTFILE 'hotstart_grid1.hst  '
 STOP
```